NEURO-FUZZY BASED FAULT DIAGNOSIS FOR NONLINEAR PROCESSES

by

Jing He

Bachelor in Electrical Engineering
Tianjin Institute of Technology, 1994

A Thesis Submitted in Partial Fulfilment of
the Requirements for the Degree of

Master of Science

in the Graduate Academic Unit of Electrical Engineering

Supervisor:	Dr. James Taylor, PhD, Electrical and Computer Engineering
Examining Board:	Dr. Rickey Dubay, PhD, Mechanical Engineering
	Dr. Christopher Diduch, PhD, Electrical and Computer Engineering
	Dr. Eugene Hill, PhD, Electrical and Computer Engineering

This thesis is accepted by the
Dean of Graduate Studies

THE UNIVERSITY OF NEW BRUNSWICK

April, 2006

To My Parents.

Abstract

Fault detection and isolation can help avoid system shutdowns, breakdowns and even catastrophes involving human fatalities and property damage. The traditional way to improve process safety and reliability is to enhance the quality and robustness of each process component. Even so, fault-free process operation cannot be guaranteed. Computational intelligence techniques are being investigated as an extension of traditional fault diagnosis methods.

In this thesis, a new approach for Neuro-Fuzzy (NF) model-based fault detection and isolation (FDI) for a nonlinear process is presented. The identification mechanism of the nonlinear dynamic process is a Neuro-Fuzzy adaptive model. We start by defining a Neuro-Fuzzy model (also called a Takagi-Sugeno type fuzzy model). This produces a nonlinear model comprised of local linear models of the process. The parameters of this model are identified by a weighted least square estimation method which is also used for symptom generation and evaluation.

This approach was successfully applied to a simulation of a Jacketed Continuously Stirred Tank Reactor (JCSTR) system. Using this technique, not only can different sensor and actuator faults be diagnosed, it can also diagnose disturbances and two faults in sequence. Furthermore, we investigate the robustness this technique applied to the JCSTR system with respect to operating point change and fault size variation, extending the robustness by developing a new nonlinear symptom mapping interpolation approach, and finally applying it to identify the fault size and type.

Acknowledgements

I would like to thank Professor James H. Taylor, my supervisor, for his many instructions during this research.

I am also thankful to Professor Maryhelen Stevenson for her guidance when I was in chaos and confusion.

Special thanks to Atalla F. Sayda, PhD Candidate share me with his knowledge and provide many useful references and friendly encouragement.

I sincerely express my appreciation to the people in my department for their kindness, support, and encouragement.

I should also thank the people in Petroleum Applications of the Wireless Systems (PAWS) Project, their support makes research like this possible.

Of course, I am grateful to my parents for their patience and *love*. Without them, this work would never have come into existence.

I also wish to thank all my friends in Canada and outside Canada for their precious friendship and confidence.

Finally, I wish thank all my stuffed animals for their consistent confidence and encouragement.

Fredericton, New Brunswick Jing He
April, 2006

TABLE OF CONTENTS

List of Tables

List of Figures

Chapter 1

Introduction

In a physical system, actuators, process components and sensors are often subjected to unexpected and unpermitted deviations from standard conditions, called faults. The basic task of fault diagnosis consists of three parts: fault detection, fault isolation, and fault identification [11].

1 Fault Detection: detection of the time of occurrence of faults in the functional units of the process, which lead to undesired or unacceptable behavior of the whole system.

2 Fault isolation: localization (classification) of different faults (faulty components).

3 Fault identification: determination of the type, magnitude and cause of the fault.

A system that includes the capacity of detecting, isolating and identifying or classifying faults is called a fault diagnosis system. Fault detection and isolation are increasing demands for man-made dynamic systems to become safer and more reliable. Model-based FDI schemes for faults are based on the deviation between measured process state outputs and estimated outputs; this approach requires accurate mathematical models of the plants. Therefore, the development of a reliable fault detection and isolation scheme for nonlinear processes is often time consuming and difficult to achieve due to the complexity of the system. Recent approaches to FDI for dynamic

systems using methods of integrating quantitative and qualitative model information are considered as an important extension to model-based FDI approaches. The trainable artificial neural network (ANN) can be used as a nonlinear dynamic model of the system, and fuzzy logic can be used together with neural networks to enhance FDI diagnostic reasoning capabilities. In this thesis, an integrated scheme, using Neuro-Fuzzy based models, provides a powerful tool to cope with nonlinear processes. This approach is successfully developed and applied to a JCSTR (Jacketed Continuously Stirred Tank Reactor) system, for diagnosis of different kinds of faults.

Chapter 2

Literature Review and Objective

2.1 Literature Review

During the last two decades, much research on FDI has been done using quantitative model-based approaches [5, 7], such as analytical approaches, parameter estimation, and residual generation. The process model is a quantitative description of the normal (fault-free) dynamic process and steady behavior, which is obtained by a well-established process modeling technique. Driven by the same process inputs, the process model must deliver a good approximation of the measured process variables, and comparing the approximated variable with the measured one yields the residual. Requiring a precise and accurate analytical model is problematic, since modeling error will affect the performance of the FDI scheme, especially in nonlinear systems representing the majority of real processes.

To circumvent this precision problem, a more suitable strategy is to use abstract qualitative models (fuzzy logic, digraphs) [9, 13]. The key advantage of fuzzy logic is that it can provide a rather transparent representation of the system, based on the linguistic interpretation in the form of IF-THEN rules, which can provide valuable information for the operator to understand the causes of faults. Using this method,

the model can deal with and analyze the data. Moreover, from these data experts can extract the rules that can be validated and combined with their prior knowledge, so more or less complete system models that describe the real process can be obtained. Unfortunately, the designer has to derive IF-THEN rules from the data sets manually. If the process is highly nonlinear, thus requiring large data sets, this is a serious limitation.

Many approaches have been considered based on ideas of computational intelligence or soft-computing by optimizing a design using artificial neural networks (ANNS) [8, 10], which provide an excellent framework for dealing with nonlinear systems. They have the ability to model nonlinear functions and provide suitable weighting factors and an appropriate architecture, and can be well trained on numerical data. However, it is not easy to incorporate heuristic knowledge from experts, due to the "black-box" characteristic. ANNS cannot give insight into the behavior of the system at the component level.

In this thesis, a robust FDI system combines both numerical (quantitative) and symbolic (qualitative) techniques, that is, Neuro-Fuzzy structures. The Neuro-Fuzzy approach represents a synergistic integration, yielding the benefits of both neural networks and fuzzy logic systems: neural networks provide a connectionist structure and learning abilities for the fuzzy logic systems, so they can model highly nonlinear systems efficiently in a fuzzy-logic format, and fuzzy logic systems provide the neural networks with high-level fuzzy IF-THEN thinking and reasoning, and a transparent mathematical structure to describe the physical relationships in the process [2, 4]. Most real-world problems are large scale and inevitably incorporate built-in uncertainties. It is frequently advantageous to use several computing techniques

synergistically rather than a single one, resulting in construction of complementary hybrid intelligent systems. Hence, Neuro-Fuzzy modeling is an integrated approach that can utilize specific techniques to construct satisfactory solutions to real-world problems.

2.2 Objective

This thesis focuses on the application of Neuro-Fuzzy techniques in FDI. It discusses the structure of the Takagi-Sugeno modeling approach. Then a Neuro-Fuzzy based learning and adaptation of the Takagi-Sugeno fuzzy model is used to diagnose faults in a JCSTR system, with faults occurring in the actuators and sensors, and also disturbances being introduced. We have extended this technique to diagnose two faults in sequence using a new approach. After that, we investigated robustness with respect to the operating point change and fault size change. Finally, we substantially improve robustness by developing a novel nonlinear mapping interpolation to identify the fault type and size from the unknown data.

Chapter 3

Basic Construction of Neuro-Fuzzy Systems

3.1 Basic Concept of Integrating Fuzzy Systems and Neural Networks

3.1.1 Common Properties of Fuzzy Systems and Neural Networks

Fuzzy systems and neural networks are both numerical model-free estimators and dynamic systems. They share the ability to capture the behavior of systems working in uncertain, imprecise, and noisy environments. Both have an advantage over traditional statistical estimation and adaptive control approaches to function estimation. They estimate a function without requiring a mathematical description of how the outputs functionally depend on the inputs.

3.1.2 Differences between Fuzzy Systems and Neural Networks

Neural networks have a large number of highly interconnected processing elements (nodes) which demonstrate the ability to learn and generalize from training patterns or data [1]. They are trainable dynamic systems which can learn a nonlinear input-output mapping from training data sets, and they can update their weights through adaptively repeating training cycles. They cannot give insight into the system, however. We know their input-output behavior, but know nothing about the system internals. Neural networks superimpose input-output samples on a "black-box" construction; is not easy to encode expert knowledge in the form of IF-THEN rules into the neural networks.

Fuzzy systems, on the other hand, are structured numerical estimators. They start from highly formalized insights about the structure of categories found in the real world and then articulate fuzzy IF-THEN rules as a kind of expert knowledge [16]. Their inputs are represented as linguistic variables, which are derived from membership functions. The membership functions map input elements into a membership grade (or membership value) in the fuzzy set. Fuzzy linguistic descriptions of the system are represented by the fuzzy IF-THEN rules. From the fuzzy implication relation we can get the consequence (conclusion) of each rule. Usually the centroid of response is used to generate the system output. However, fuzzy systems encounter different difficulties, such as how to determine the fuzzy logic rules and the membership functions.

3.1.3 Reason for Integrating Fuzzy Systems and Neural Networks

Fuzzy logic and neural networks are complementary technologies. The neuro-fuzzy synergistic integration reaps the benefits of both neural networks and fuzzy logic systems. Neural networks have good learning, computation, and optimization capabilities. They can automatically tune the parameters of fuzzy rules and membership functions from the training data set, thus improving the performance of fuzzy systems. Fuzzy systems can deal with issues such as reasoning and encode the expert knowledge on a higher level, thus improving the transparency and performance of neural networks, providing a structure framework to the neural networks. In this way, we can combine the learning and computational ability of neural networks with the human like IF-THEN thinking and reasoning of fuzzy system, to integrate them.

3.2 Construction of Fuzzy Systems and Neural Networks

3.2.1 Basic Concept of Neuro-Fuzzy Systems

This Neuro-Fuzzy model can be considered to be a neural network realization of the Takagi-Sugeno-Kang fuzzy inference model (TSK model) [14, 15]. The basic idea of using neural networks to realize or generalize the TSK model is to implement the membership functions in the preconditions as well as the inference function in the consequents. This approach can solve two main problems in fuzzy reasoning: the lack of a definite method for determining the membership functions and the lack of a learning function for self-tuning inference rules. The neural networks in the precondition component can learn the proper membership functions, and those in the

consequent component learn the proper "action" of a rule. These fuzzy rules are characterized by a collection of fuzzy IF-THEN rules in which the preconditions and consequents involve linguistic variables. This collection of fuzzy rules characterizes the simple input-output relation of the system. The general form of a fuzzy rule R_i in the case of the multi-input-single-output (MISO) system is:

IF $x_1(k)$ is $A_{i,1}$ and $x_2(k)$ is $A_{i,2}$ and $\ldots$, x_n is $A_{i,n}(k)$

THEN $f_i(k) = \omega_{0,i} + \omega_{1,i}x_1(k) + \omega_{2,i}x_2(k) + \cdots + \omega_{n,i}x_n(k)$

where R_i means the i^{th} implication, $i \in 1, \ldots, r$. The variables $x_1, \ldots, x_n$ comprise the input vector, $\omega_{0,i}, \omega_{1,i}, \ldots, \omega_{n,i}$ are the consequent parameters, $A_{i,1}, \ldots, A_{i,n}$ are the fuzzy sets defined on the universe of discourse of the inputs (also called antecedent parameters), and $f_i(k)$ is the output from the i^{th} implication.

The fuzzy implications are formed by fuzzily partitioning the inputs space. Therefore, the premise of a fuzzy implication indicates a fuzzy subspace of the inputs space. Each implicational relation expresses a local input-output relation. We can see that those implicational relations express highly nonlinear functional relations.

The identification of a fuzzy model using input-output data consists of two parts: structure identification and parameter identification. Structure identification consists of premise structure identification and consequent structure identification. Regarding the the premise structure, we need to find which variables are necessary in the premise. We also need to find out the optimal fuzzy partition of the input space, where the number of fuzzy subspaces corresponds to that of the necessary implications. The second procedure is concerned with consequent structure identification. We need to find which variables are necessary in the consequent of an implication. In addition, we also need to find a criterion for the verification of an obtained structure.

The methods for identifying nonlinear models are the following: in the presence of moderate noise, the parameters of the model with the true structure are the least sensitive to the changes of the observed data, which are used for identifying the parameters.

Parameter identification also consists of premise parameter identification and consequent parameter identification. Premise parameters are the fuzzy variables of the membership function. We can use different optimization techniques to identify them. Sugeno [14] suggests a successive identification algorithm: as a piece of input-output data is processed, we adjust the parameters so that the error of the inferred output decreases, where the parameters are those that have been estimated by using the past data. The consequent parameters are the coefficients of linear equations. When a set of input-output data is given, the consequent parameters can be identified by, for example, the least squares method.

3.2.2 Basic Structure of a Neuro-Fuzzy System

We consider the i^{th} rule of a first-order Takagi-Sugeno fuzzy system in Figure 3.1 consisting of n inputs and r rules:

Layer 1: Every node in this layer is an adaptive node with a node membership function $\mu_{Aij}(x_k)$, where $i \in \{1, \ldots, r\}, j \in \{1, \ldots, n\}$, where x is the input to the node, and Aij is the linguistic label associated with this node. There are various forms of membership function for the fuzzy set Aij. We can choose any continuous piecewise differentiable functions, such as the commonly used trapezoidal, triangular, or bell shaped membership functions.Parameters in this layer are referred to as premise parameters.

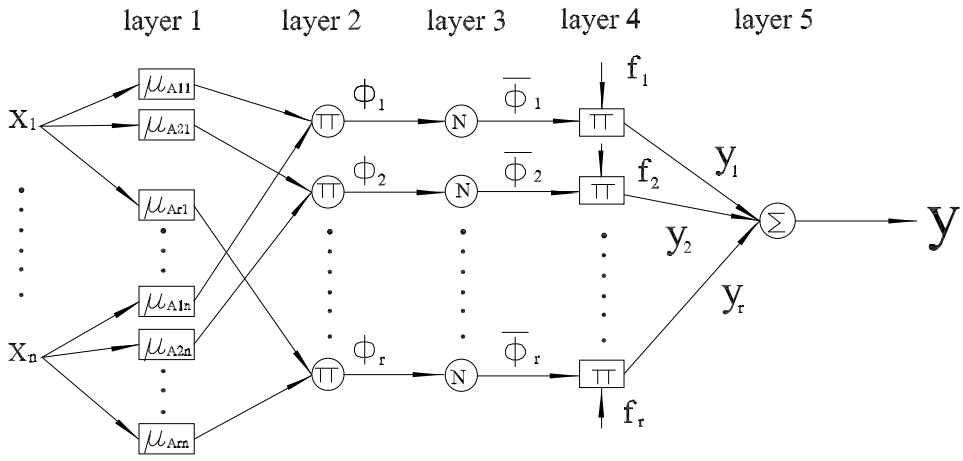

Figure 3.1: The Basic Structure of a Neuro-Fuzzy System

The building of fuzzy membership functions need satisfy the following requirements:

1. Membership functions reaching to plus and minus infinity must exist.

2. The sum of the membership function values should add up to 1 for all symptom values.

These conditions are necessary in order to ensure the intuitive understanding of membership functions. Figure 3.2 displays a typical set of symmetric triangular membership functions, and equation (3.1) describes one example.

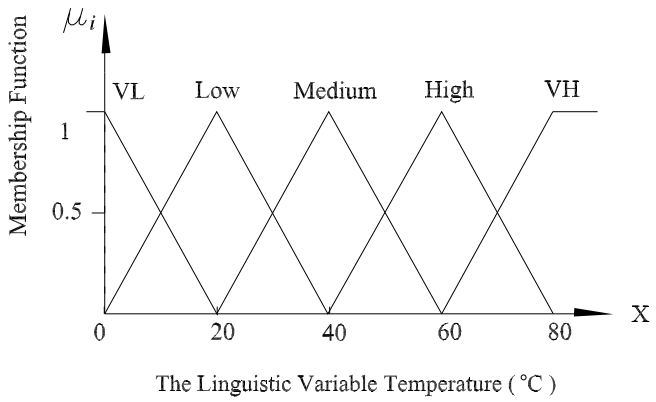

Figure 3.2: Membership Functions Based on Triangles

$$\mu_i = \begin{cases} 0 & x \leqq a \\ \frac{x-a}{b-a} & a \leq x \leq b \\ \frac{c-x}{c-b} & b \leq x \leq c \\ 0 & c \leqq x \end{cases} \tag{3.1}$$

The above $[a, b, c]$ is the parameter set of the triangular membership function, where a is the membership function's left intercept with grade equal to 0, b is the center peak where the grade equals 1, and c is the right intercept at grade equal to 0. The universe of discourse X comprises the crisp values from 0 to 80, with fuzzy values: VL (very low), Low, Medium, High, and VH (very high). In Figure 3.2, the linguistic value "Medium", where $a = 20, b = 40, c = 60$, is defined over the universe of discourse $X = [0 : 80]$.

Layer 2: Every node in this layer is a fixed node labeled $\prod$, which multiplies the incoming signals and sends the product out:

$$\Phi_i = \prod_{j=1}^{n} \mu_{Aij}(x_j) \tag{3.2}$$

where $i \in \{1, \ldots, r\}, j \in \{1, \ldots, n\}$. Each node output represents the firing strength of a rule.

Layer 3: Every node in this layer is a fixed node labeled N. The i^{th} node calculates the ratio of the i^{th} rule's firing strength to the sum of all rules' firing strengths:

$$\overline{\Phi_i} = \frac{\Phi_i}{\sum_{k=1}^{r} \Phi_k} \tag{3.3}$$

For convenience, outputs of this layer are called normalized firing strengths.

Layer 4: Every node in this layer is an adaptive node with a node function:

$$y_i = \overline{\Phi_i} f_i \tag{3.4}$$

$$f_i(k) = \omega_{0,i} + \omega_{1,i} x_1(k) + \omega_{2,i} x_2(k) + \cdots + \omega_{n,i} x_n(k) \tag{3.5}$$

where $\overline{\Phi_i}$ is a normalized firing strength from layer 3 and $\omega_{0,i}, \omega_{1,i}, \ldots, \omega_{n,i}$ are referred to as consequent parameters.

Layer 5: The single node in this layer is a fixed node, which computes the overall output as the summation of all incoming signals:

$$y = \sum_{i=1}^{r} \overline{\Phi_i} f_i = \sum_{i=1}^{r} y_i \tag{3.6}$$

Chapter 4

Neuro-Fuzzy Systems Approaches in FDI

4.1 Introduction

Most FDI schemes consist of two major levels: a symptom generation level and a diagnostic level. In the first one, symptoms are generated which indicate the state of the process and enable fault detection. In the second, the most probable fault is identified. Generating significant symptoms is important: the better the symptoms are, the more successful the diagnosis will be. In the following, a new approach using neural networks and fuzzy-models is developed and demonstrated on an industrial JCSTR (Jacketed Continuously Stirred Tank Reactor) system. The scheme is based on the comparison of actual process variables with nominal ones, derived from the process model. The symptoms are generated with the nonlinear Neuro-Fuzzy model that is run in parallel to the process. In this technique, a fairly transparent FDI scheme for nonlinear processes is presented, which has the following advantages:

1. Several symptoms can be generated from the model, based on its intuitive structure and the parameters. It is possible to distinguish different faults in all regions of operation.

2. The laborious modeling task for nonlinear systems is reduced. The model can be trained from measured data, and less prior knowledge is required.

This technique is based on a Takagi-Sugeno fuzzy model [14] of the nominal process. The models can be built from heuristic knowledge and by means of identification algorithms from measurement data. We use the Local Linear Model Tree Algorithm (LOLIMOT) [3] for diagnosis. This approach is capable of determining the structure of the fuzzy system as well as the parameters of the rule consequent parts. After the structure is determined, the parameters of the rule consequents can be estimated by a weighted linear least squares algorithm.

4.2 Neuro-Fuzzy Functional Model

Nonlinear dynamic models are the basis for sophisticated control and fault diagnosis systems. For dynamic processes, Takagi-Sugeno fuzzy models are especially attractive because their rule consequents can be interpreted as linear difference equations that represent local poles, zeros, gains, etc. The fuzzy functional model approximates a nonlinear dynamic process by piece-wise linear models as shown in Figure 4.1 [6]. Each local model is valid in a sub-region of the input space. The partitions where the local models are valid are not crisp, but fuzzy. Therefore the validity of one local model for a certain point in the input space is expressed by a weighting function continuously defined over the whole input space and scaled from zero (not valid) to one (fully valid). The model output is computed as a weighted sum of all local models (hyperplanes). This process leads to a nonlinear interpolation between the local model outputs. The rule consequents describe the fuzzy regions in the input space. The rule consequents are crisp functions of the model inputs.

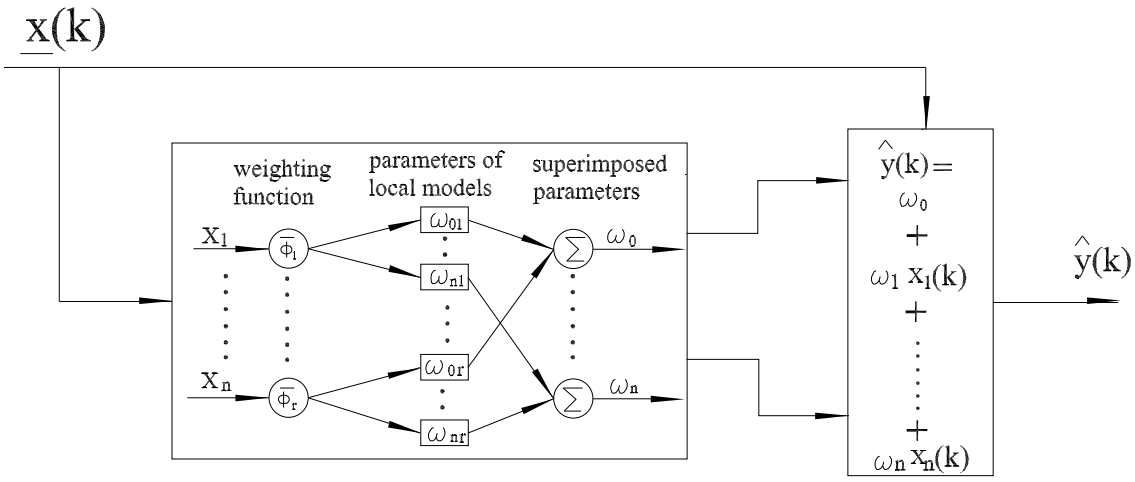

Figure 4.1: Structure of Local Linear Model

The nonlinear dynamic discrete function f with n inputs x_i, $i = 1, \cdots, n$ and one output $\hat{y}$ is defined as

$$\hat{y}(k) = f(\underline{x}(k)) \tag{4.1}$$

$$\begin{aligned} \underline{x}(k) &= [x_1(k), \ldots, x_n(k)] \\ &= [u_1(k-1), \ldots, u_1(k-n_{u1}), \ldots, u_m(k-1), \ldots, u_m(k-n_{um})] \end{aligned} \tag{4.2}$$

Note that $\underline{x}(k)$ includes all inputs (process inputs and disturbances), and their time delayed values. The unknown function $f(.)$ is approximated by a piece-wise linear model, in the form of a Takagi-Sugeno fuzzy model.

Rule R_i: IF $x_1(k)$ is $A_{i,1}$, AND $x_2(k)$ is $A_{i,2}$, AND $\ldots x_n(k)$ is $A_{i,n}$, THEN

$$\hat{y}_i(k) = \omega_{0,i} + \omega_{1,i}x_1(k) + \omega_{2,i}x_2(k) + \ldots + \omega_{n,i}x_n(k) \tag{4.3}$$

where $i \in 1, \ldots, r$, $x_1, \ldots, x_n$ are the input vector elements, and $A_{i,1}, \ldots, A_{i,n}$ are the fuzzy sets defined on the universe of discourse of the inputs (also called antecedent

parameters). The parameters $\omega_{0,i},\ \omega_{1,i},\ldots,\ \omega_{n,i}$ are consequent parameters of the i^{th} linear regression model, which can be found by a weighted least squares estimation method. The output of the overall model is the weighted sum of all r local linear model parameters,

$$\hat{y}(k) = \sum_{i=1}^{r} f_i(k)\overline{\Phi_i} \tag{4.4}$$

where $\overline{\Phi_i}$ is the normalized weighting function for the i^{th} model. In the sequel, for the sake of simplicity, the equation can also be written in the form:

$$\begin{aligned} \hat{y}(k) &= (\sum_{i=1}^{r} \omega_{0,i}\overline{\Phi_i}) + (\sum_{i=1}^{r} \omega_{1,i}\overline{\Phi_i})x_1(k) + \ldots + (\sum_{i=1}^{r} \omega_{n,i}\overline{\Phi_i})x_n(k) \\ &= (\omega_0 + \omega_1 x_1(k) + \omega_2 x_2(k) + \ldots + \omega_n x_n(k)) \end{aligned} \tag{4.5}$$

where each parameter ω_i is a nonlinear interpolation between the parameters of the rule conclusions. This process is referred to as dynamic linearization (linearization along a trajectory). The superimposed parameters ω_i describe the dynamic process behavior near the actual set point. The dynamic linearization has some appealing advantages compared to normal linearization: Linearized Takagi-Sugeno fuzzy models cope with errors which are caused by the rule premise part, while normal linearized models do not. Dynamic linearization overcomes this disadvantage. The characteristic values can be calculated as the weighted superimposition of the rule consequent parameters, and the disturbing influence of the rule premise part is minimized.

4.3 Fault Detection Symptom Generation

4.3.1 Concept of a Residual

As mentioned above, the local linear model is well suited for generation of symptoms used for FDI purposes. One typical symptom type is the deviation between measured and estimated signals, the so called output residuals r. They have the property of being close to zero in the fault free case and significantly deviating from zero if a fault affects the true process or the process measurements. They are generally not exactly zero, due to uncertainty and / or noise.

This only applies under the ideal conditions of having an accurate model and uncorrupted measurements. However, in practice, due to modeling uncertainty and measurement noise, it is necessary to assign thresholds δ larger than zero in order to avoid false alarms. This is associated with a reduction of fault detection sensitivity, and with this choice of the threshold only a compromise between decision sensitivity and false alarm rate can be achieved [5].

4.3.2 Residual-Based Symptoms

The symptoms are based on the comparison of features from the process behavior with nominal features from the model. In Figure 4.2, d_a represents actuator faults, d_s represents sensor faults, d_p represents process disturbances, u represents the actual input vector, u_d represents the vector of desired inputs, y_d represents the desired process outputs, y represents the actual process output, and $\hat{y}$ represents the Neuro-Fuzzy model output. The simplest symptom is the output error between the model and the process, with the time window of appropriate length l and the threshold δ [6].

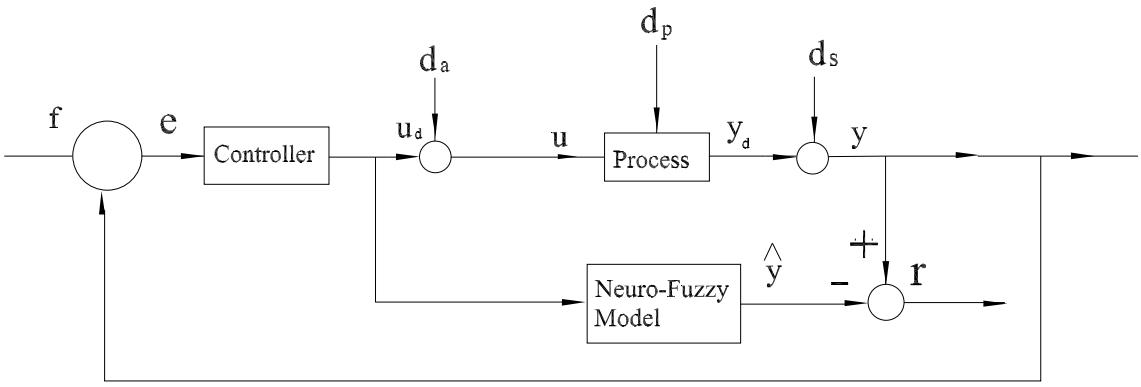

Figure 4.2: Symptom Generation Using a Neuro-Fuzzy Model

$$r_k = \sum_{i=1}^{l} |\hat{y}(k-i) - y(k-i)| \tag{4.6}$$

IF $r_k < \delta$ there is no fault

IF $r_k \geq \delta$ there is fault

4.4 Fault Diagnosis-Symptom Evaluation

The fault symptom patterns generated by the residual, as described above, are simple and lead to an easy approach for diagnosis. For detection, the residual generated using the fault-free Neuro-Fuzzy model NF_0 becomes large in magnitude when an anomaly occurs, so detection is fast and certain.

Once detection is achieved, the Neuro-Fuzzy models $NF_j, j = 1, 2, .., 10$ are monitored and the resulting ten output patterns $\hat{y}_j$ are compared with the outputs of the process. The output patterns are unique for each anomaly, so isolation is achieved when one of the $\hat{y}_j$ patterns matches that of the process; in other words, the residual $r_j = y - \hat{y}_j$ is small (nearly equal to zero), i.e, it is within the threshold δ. This procedure is described in more detail and illustrated in section 5.5.

Chapter 5

Single Fault Diagnosis in a JCSTR System

5.1 Introduction to the JCSTR System

5.1.1 Process Description

Consider a jacketed stirred tank reactor and heater as shown in Figure 5.1, where the tank inlet stream is received from another process unit. The objective is to raise and maintain the temperature of the contents of the tank to a desired value. A heat transfer fluid is circulated through a jacket to heat the fluid in the tank. In some processes, steam is used as the heat transfer fluid, and most of the energy exchanged is due to the phase change of steam to water. In other processes, a heat transfer fluid is used where there is no phase change. In this module, we assume that no change of phase occurs in either the tank fluid or the jacket fluid. This model was developed by Atalla F. Sayda [12] and is presented in more detail in Appendix A.

As shown in Figure 5.1, the JCSTR system has the following five input variables

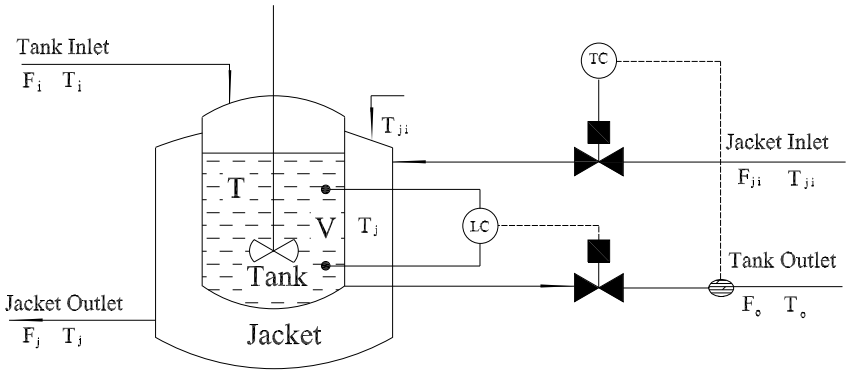

Figure 5.1: Jacketed Continuously Stirred Tank Reactor (JCSTR)

which are denoted by u:

1. F_{out}: Mix Outflow

2. F_{jin}: Jacket Heating Fluid Inflow

3. F_{in}: Mix Inflow Disturbance

4. T_{in}: Inlet Temperature Disturbance

5. T_{jin}: Jacket Heating Fluid Temperature Disturbance

It also has the following three outputs variables which are denoted by y:

1. T_J: Measured Heating Fluid Temperature

2. T_T: Measured Mix Temperature

3. V_T: Measured Volume

Table 5.1 shows the process output data in the nominal case defined by a volume set point $V_{sp} = 180\,m^3$ and temperature set point $T_{sp} = 33.5824\,°C$. Each variable

has a pair of values which indicate the minimum and maximum value. In the nominal (steady state) case these are equal.

Number	Outputs	Variables	Data	Unit
1	Heating Fluid Temperature	T_{J0}	[104.2784104.2784]	$°C$
2	Measured Mix Temperature	T_{T0}	[33.5824 33.5824]	$°C$
3	Measured Volume	V_{T0}	[180 180]	m^3

Table 5.1: Process Output Data of the Nominal Case

Table 5.2 shows the process input data in the nominal case. Each variable has a pair of values which indicate the minimum and maximum value in the nominal. Again, for each variable, all the data pairs are the same.

Number	Inputs	Variables	Data	Unit
1	Mix Outflow	F_{out}	[0.1000 0.1000]	m^3/s
2	Heating Fluid Inflow	F_{jin}	[0.1500 0.1500]	m^3/s
3	Mix Inflow Disturbance	F_{in}	[0.1000 0.1000]	m^3/s
4	Inlet Temperature Disturbance	T_{in}	[283 283]	K
5	Heating Fluid Temperature Disturbance	T_{jin}	[393 393]	K

Table 5.2: Process Input Data of the Nominal Case

5.1.2 Objective

The objective is to control the temperature and the volume inside the tank by varying the jacket inlet valve flow rate (the temperature control or TC loop) and tank outlet valve flow rate (the level control or LC loop) respectively. A set of faults and disturbances was chosen to study the behavior of the JCSTR based on a nonlinear model which is described in Appendix A. The disturbances and fault set can be summarized by the following a list of anomalies:

1. Disturbance = 'Low Mix Inflow': -50 percent anomaly;
2. Disturbance = 'High Mix Inflow': 50 percent anomaly;
3. Disturbance = 'Low Inlet Temperature': -50 percent anomaly;
4. Disturbance = 'High Inlet Temperature': 50 percent anomaly;
5. Disturbance = 'Low Heating Fluid Temperature': -20 percent anomaly;
6. Disturbance = 'High Heating Fluid Temperature': 20 percent anomaly;
7. Fault = 'Faulty Temperature Sensor': -20 percent fault;
8. Fault = 'Faulty Volume Sensor': -20 percent fault ;
9. Fault = 'Faulty Outflow Valve': -20 percent fault;
10. Fault = 'Faulty Heating Fluid Inflow Valve': 20 percent fault.

5.2 Anomaly Models

The specific form of anomalies considered in this study are indicated in Figure 4.2:

1. An actuator failure is represented by an additive error signal d_a introduced in the output of the controller. For example, if the controller is calling for a value to be 80 percent open and there is a "-20 percent fault", then the valve is actually 64 percent open. We choose to model this as an additive input $d_a = -16$ percent; however the same effect would result if an artificial "actuator gain" were set to 0.8.

2. A sensor failure is represented by an additive error signal d_s introduced in the output of the process. For example, if the actual process temperature is $100\,°C$ and there is a "-20 percent fault ", then the temperature sensor reading is $80\,°C$. Again, we choose to model this as an additive input $d_s = -20\,°C$; however the same effect would result if an artificial "sensor gain" were to set to 0.8.

3. Disturbances represent uncontrolled inputs to the process (inputs not involved in closed-loop control) changing by a certain percent. For example, if the mixture inflow is nominally $F_{in} = 0.1\,m^3/s$ then a "-20 percent disturbance" is a step change from $0.1\,m^3/s$ to $0.08\,m^3/s$.

5.3 Learning in the Neural-Fuzzy Model

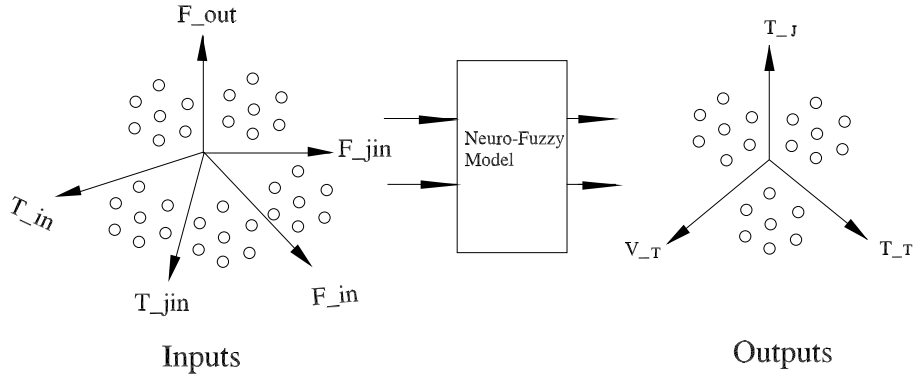

Figure 5.2: Neuro-Fuzzy Model Input and Output Map

We consider a number of scenarios which happen from hour 0 to hour 5. In Figure 4.2, there are five inputs $u = [F_{out}; F_{jin}; F_{in}; T_{in}; T_{jin}]$. For each input, we choose one

datum from every ten generated data points. These data are applied to the JCSTR system, producing three corresponding outputs $y = [T_J; T_T; V_T]$. The same input data are also applied to the Neuro-Fuzzy system, producing three corresponding outputs $\hat{y}$. This training process produces a steady-state map shown in Figure 5.2, in which the *circle* variables indicate the input and output data. When the system is in the normal condition, we build the fault-free Neuro-Fuzzy model denoted by NF_0. We train the NF_0 model to produce its corresponding output variables in the normal condition. When the system is in faulty conditions (anomalies 1 to 10), we also build Neuro-Fuzzy faulty models NF_1 to NF_{10} for these cases. We also train each of these faulty-models to produce its corresponding output variables for nominal-sized anomalies. The Neuro-Fuzzy learning approach relies on the off-line weighted least square estimation method. In neural learning, an objective function E is sought to be minimized:

$$E = \frac{1}{2}(y - \hat{y})^2 \tag{5.1}$$

We can optimize the consequent parameters ω_i to reduce the error measure E between the Neuro-Fuzzy model output $\hat{y}$ and the process output y. The learning rule for ω_i is:

$$\omega_i(t+1) = \omega_i(t) + \alpha \prod_{j=1}^{5} \mu_{Aij}(x_j)\, u\, (y - \hat{y})^T \tag{5.2}$$

where t is the number of iteration of learning, α is the constant learning rate, u is the vector of input variables, $\mu_{Aij}(x_j)(\ i \in \{1, \ldots, r\}, j \in \{1, \ldots, n\})$ are the membership functions, of triangular form, equation (3.1). There are three objectives: The first is to train and test the performance of the Neuro-Fuzzy model in the fault-free condition, the second is to detect the anomalies, and the third is to isolate the anomalies after they occur.

5.4 Fault-free Behavior of the Neuro-Fuzzy Model

In this section, we set different operating points for the measured volume and measured mix temperature variables while the system is fault-free. Figure 5.3 shows the two "staircase" plots which indicate the NF fault-free (NF_0) model outputs corresponding to different operating point changes. In the figures, the *star* variables indicate the process outputs under normal conditions, and the *circle* variables indicate the Neuro-Fuzzy model outputs under normal conditions.

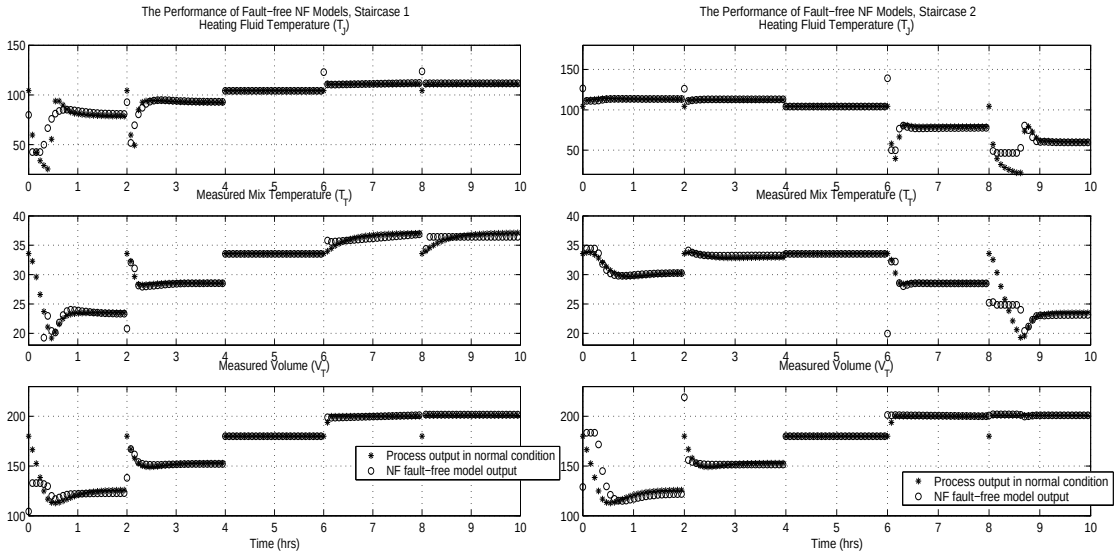

(a) Staircase 1 (b) Staircase 2

Figure 5.3: The Fault-free Performance of the Neuro-Fuzzy Model

5.4.1 The First "Staircase" Plot

Figure 5.3 (a) shows the NF fault-free model outputs for the first "staircase".

1. From hour 0 to hour 2, the operating points of both variables are set at -30 percent ($[dV_{sp}, dT_{sp}] = [-54\,m^3, -10.5\,^\circ C]$): from hour 0.3, the NF fault-free model outputs gradually fit the process model outputs and reach almost the

same steady state.

2. From hour 2 to hour 4, the operating points of both variables are set at -15 percent ($[dV_{sp}, dT_{sp}] = [-27\,m^3, -5.25\,°C]$): from hour 2.1, the NF fault-free model outputs gradually fit the process model outputs and reach the same steady state.

3. From hour 4 to hour 6, the operating points of both variables are nominal ($[dV_{sp}, dT_{sp}] = [0, 0]$): from hour 4.0, the NF fault-free model outputs immediately fit the process model outputs so that they overlap each other. So there are six straight lines, not three straight lines in the figure.

4. From hour 6 to hour 8, the operating points of both variables are set at 15 percent ($[dV_{sp}; dT_{sp}] = [27\,m^3, 5.25\,°C]$): from hour 6.1, the NF fault-free model outputs gradually fit the process model outputs and reach the same steady state.

5. From hour 8 to hour 10, the operating points of both variables are set at 30 percent ($[dV_{sp}, dT_{sp}] = [54\,m^3, 10.5\,°C]$): from hour 8.2, the NF fault-free model outputs gradually fit the process model outputs and reach the same steady state.

Figure 5.3 (a) shows that the NF fault-free model outputs for "staircase 1" provide a good steady state match with the process model outputs, so the NF fault-free model should have good performance.

5.4.2 The Second "Staircase" Plot

In a similar study, Figure 5.3 (b) shows the NF fault-free model outputs for the second "staircase": From hour 0 to hour 2, the operating point of the measured volume is set at -30 percent and the measured mix temperature is set at 30 percent ($[dV_{sp}, dT_{sp}] = [-54\,m^3, 10.5\,°C]$); from hour 2 to hour 4, the operating point of the measured volume is set at -15 percent and the measured mix temperature is set at 15 percent ($[dV_{sp}, dT_{sp}] = [-27\,m^3, 5.25\,°C]$); from hour 4 to hour 6, the operating points of both variables are nominal ($[dV_{sp}, dT_{sp}] = [0, 0]$); from hour 6 to hour 8, the operating point of the measured volume is set at 15 percent and measured mix temperature is set at -15 percent ($[dV_{sp}; dT_{sp}] = [27\,m^3, -5.25\,°C]$); from hour 8 to hour 10, the operating point of the measured volume is set at 30 percent and measured mix temperature is set at -30 percent ($[dV_{sp}, dT_{sp}] = [54\,m^3, -10.5\,°C]$). Again, Figure 5.3 (b) shows that the NF fault-free model outputs for "staircase 2" also provide a good steady-state match with the process model outputs.

5.5 Diagnosis of Single Anomalies

5.5.1 Procedure

In this study, we develop and test our approach for diagnosing one anomaly (fault or disturbance) may occur in the JCSTR system. We train the Neuro-Fuzzy models and see how they can diagnose these ten anomalies after they occur. We set the setpoint of the measured volume and measured mix temperature to two different values to test the robustness of the NF model. A few figures are included in the body of this thesis to illustrate the process, and the rest are included in Appendix B.

5.5.2 Using the Neuro-Fuzzy Model in the Nominal Case

In this case, the normal operating point of the volume and temperature are nominal ($dV_{sp} = 0, dT_{sp} = 0$). The system starts in a fault-free condition, and an anomaly is introduced at hour 2. Data are acquired from hour 0 to hour 5 for fault detection and isolation testing at the rate of $0.6\, sample/min$.

1 Fault Detection Stage

All ten anomalies are displayed in the figure and tables that follow. Two of these anomalies are discussed as examples to illustrate the detection stage, and the other anomalies are attached in Appendix B. From the results, all the anomalies can be detected if they occur one at a time. In Figure 5.4, the *plus* variables indicate the NF model outputs under normal conditions, and the *star* variables indicate the system process outputs in faulty conditions.

Figure 5.4 (a) shows the effect of a low mix inflow disturbance which decreases by 50 percent at hour 2 . The heating fluid temperature decreases by 35 percent, the measured mix temperature increases by 7 percent and then returns to normal condition, and the measured volume decreases by 8 percent and then returns to normal. Thus, all of the three output variables have changes.

Figure 5.4 (b) shows the effect of a faulty temperature sensor which decreases by 20 percent at hour 2 . The heating fluid temperature increases by 6 percent, the measured mix temperature decreases by 20 percent, and the measured volume has no change. Two of the output variables have changes.

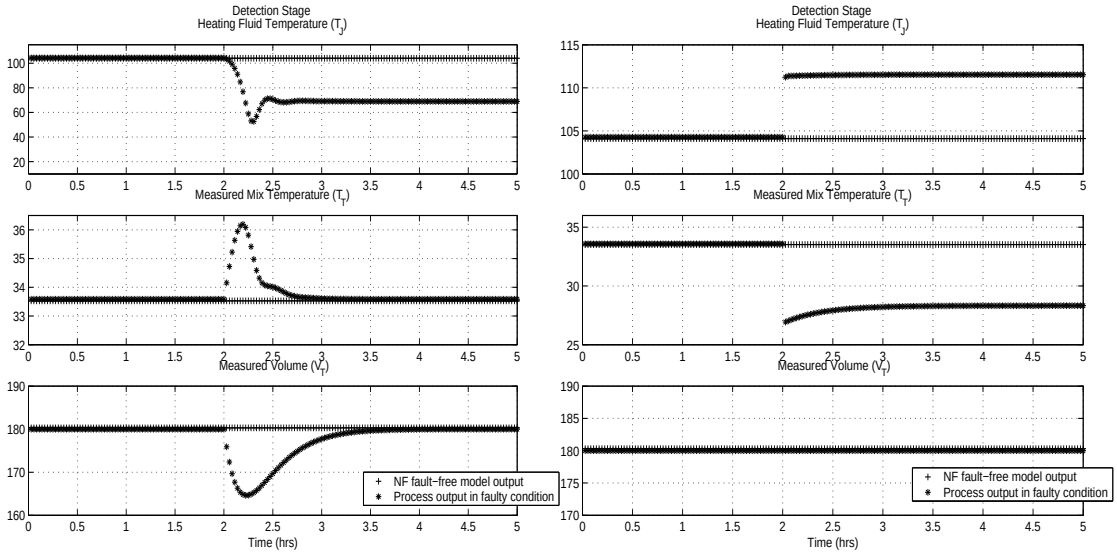

(a) Anomaly 1 (b) Anomaly 7

Figure 5.4: Anomaly Detection in the Nominal Case

In the detection stage, from hour 0 to hour 2, the Neuro-Fuzzy model is in the normal condition, so there is no anomaly in the system. Based on the fault-free Neuro-Fuzzy model NF_0, we detect an anomaly in the system soon after hour 2. Some other results are attached in Appendix B.

2 Fault Isolation Stage

In the isolation stage, from hour 2 to hour 5, we use a bank of Neuro-Fuzzy faulty models NF_1 to NF_{10} (which are developed offline) to isolate each of the ten anomalies.

In Figure 5.5 to Figure 5.9, the *plus* variables indicate the NF model outputs in normal conditions, the *circle* variables indicate the NF model outputs in faulty conditions, and the *solid* variables indicate the system process outputs in faulty

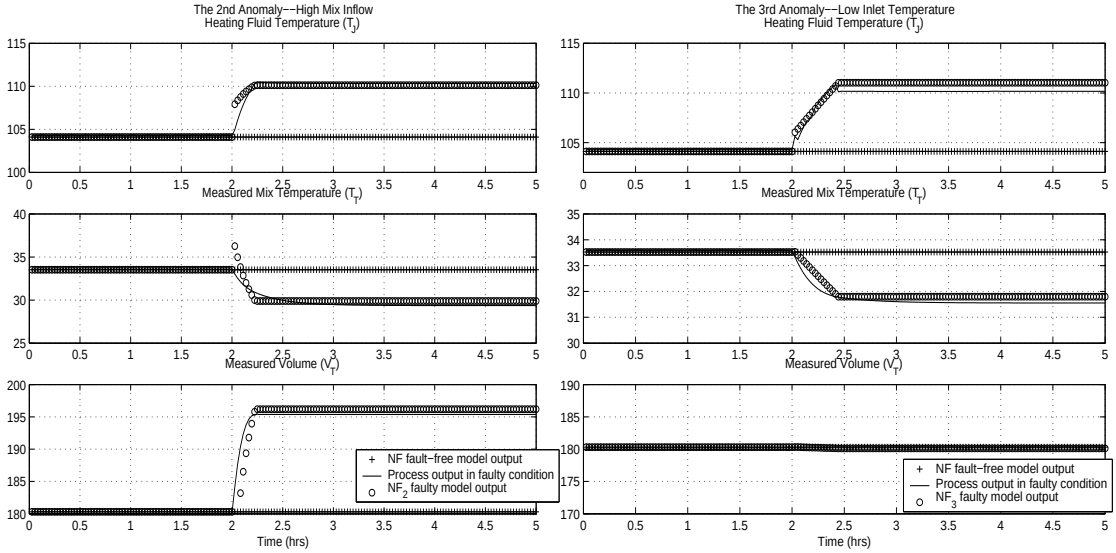

(a) Anomaly 2 (b) Anomaly 3

Figure 5.5: Anomaly Isolation Stage 1 in Nominal Case

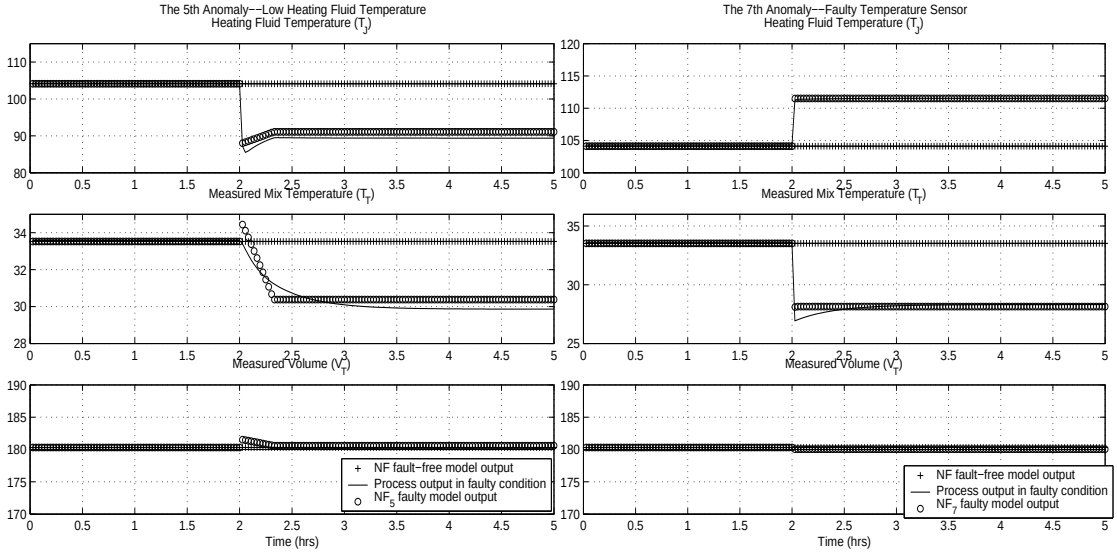

(a) Anomaly 5 (b) Anomaly 7

Figure 5.6: Anomaly Isolation Stage 1 in the Nominal Case

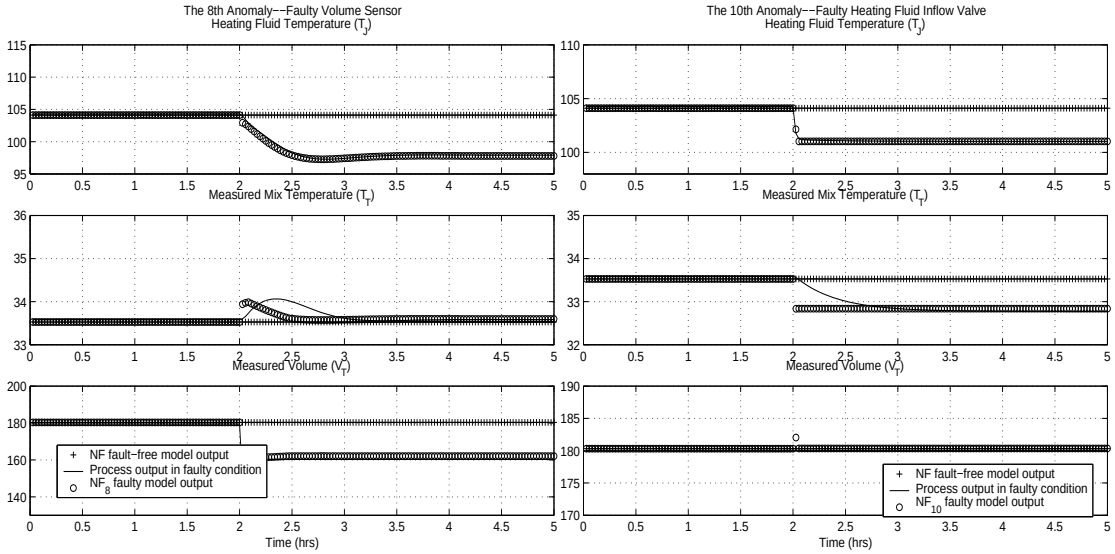

(a) Anomaly 8 (b) Anomaly 10

Figure 5.7: Anomaly Isolation Stage 1 in the Nominal Case

conditions. The solid variables are used to determine whether NF faulty models have good performance.

Table 5.3 and Table 5.4 show the two isolation stages and results, using the Neuro-Fuzzy models. For the three output variables, each variable has a pair of values which constitute the "symptoms" used for isolation, as discussed below. Note that the "threshold" and "range" used in categorizing symptoms below were determined by the operating range of each variable and the need to minimize false alarms.

For the heating fluid temperature, $T_{J0} = 104.1092\,^{\circ}C$ is the value in normal conditions, and other values of $P(T_J)$ are recorded, namely the minimum (T_{Jmin}) or maximum (T_{Jmax}) values in the faulty condition. We define $\Delta P(T_J) = T_{Jmax} - T_{J0}$ or $\Delta P(T_J) = T_{J0} - T_{Jmin}$, accordingly. The threshold ($\delta(T_J)$) for the normal condition is determined to be $3\,^{\circ}C$, i.e, a value within

'$\pm 3\,°C$' indicates that the output is normal, and its pattern is denoted by '0'. When $\Delta P(T_J)$ value is above or below the threshold $3\,°C$, an anomaly in the system is detected. The range ($\Lambda(T_J)$) of different degrees is determined to be $16\,°C$. If $\Delta P(T_J)$ value is between '$3°C$' and '$19\,°C$', its pattern is denoted by '+'. If $\Delta P(T_J)$ value is between '$19\,°C'$ and '$35\,°C$', its pattern is denoted by '++', and so on. If $\Delta P(T_J)$ value is between '$-19\,°C$' and '$-3\,°C$', its pattern is denoted by '−'. If $\Delta P(T_J)$ value is between '$-35\,°C$' and '$-19\,°C$', its pattern is denoted by '−−', and so on.

For the measured mix temperature, $T_{T0} = 33.5265\,°C$ is the value in normal conditions, and other values of $P(T_T)$ are recorded, namely the minimum (T_{Tmin}) or maximum (T_{Tmmax}) values in the faulty condition. We define $\Delta P(T_T) = T_{Tmax} - T_{T0}$ or $\Delta P(T_T) = T_{T0} - T_{Tmin}$, accordingly. The threshold ($\delta(T_T)$) for the normal condition is determined to be $1\,°C$, a value within '$\pm 1\,°C$' indicates that the output is normal, and its pattern is denoted by '0'. When $\Delta P(T_T)$ value is above or below the threshold $1\,°C$, an anomaly in the system is detected. The range ($\Lambda(T_T)$) of different degrees is determined to be $4\,°C$. If $\Delta P(T_T)$ value is between '$1\,°C$' and '$5\,°C$', its pattern is denoted by '+'. If $\Delta P(T_T)$ value is between '$5\,°C$' and '$9\,°C$', its pattern is denoted by '++', and so on. If $\Delta P(T_T)$ value is between '$-5\,°C$' and '$-1\,°C$', its pattern is denoted by '−'. If $\Delta P(T_T)$ value is between '$-9\,°C$' and '$-5\,°C$', its pattern is denoted by '−−', and so on.

For the measured volume, $V_{T0} = 180.3020\,m^3$ is the value in normal conditions, and other values of $P(V_T)$ are recorded, namely the minimum (V_{Tmin}) or maximum (V_{Tmax}) value in the faulty condition. We define $\Delta P(V_T) = V_{Tmax} - V_{T0}$

or $\Delta P(V_T) = V_{T0} - V_{Tmin}$, accordingly. The threshold ($\delta(V_T)$) for the normal condition is determined to be $5\,m^3$, i.e. a value within '$\pm 5\,m^3$' indicates that the output is normal, and its pattern is denoted by '0'. When $\Delta P(V_T)$ value is above or below the threshold $5\,m^3$, an anomaly in the system is detected. The range ($\Lambda(V_T)$) of different degrees is determined to be $16\,m^3$. If $\Delta P(V_T)$ value is between '$5\,m^3$' and '$21\,m^3$', its pattern is denoted by '+'. If $\Delta P(V_T)$ value is between '$21\,m^3$' and '$37\,m^3$', its pattern is denoted by '++', and so on. If $\Delta P(V_T)$ value is between '$-21\,m^3$' and '$-5\,m^3$', its pattern is denoted by '−'. If $\Delta P(V_T)$ value is between '$-37\,m^3$' and '$-21\,m^3$', its pattern is denoted by '−−', and so on.

Thus, in Table 5.3 to Table 5.4, those patterns are denoted by '0', '−', '−−', '− − −', '+', '++', and '−⇒0' based on the behavior of '*unchanged*', '*decreases to low degree*', '*decreases to very low degree*', '*decreases to very very low degree*', '*increases to high degree*', '*increases to very high degree*', and '*increases from low degree to normal condition*' symptoms.

Returning to Figure 5.5 to Figure 5.7 and Table 5.3, we see that during the first isolation stage can isolate the 2nd, 3rd, 5th, 7th, 8th, and 10th anomalies by hour 2.1.

Figure 5.8 to Figure 5.9 and Table 5.4 show the second isolation stage. By hour 2.5, the three output variables for the last four anomalies have different patterns and sizes. We can isolate the 1st, 4th, 6th, and 9th anomalies within 30 minutes.

Fault Isolation, Stage 1						
	Heating Fluid Temperature $P(T_J) = [\,T_{J0} \quad T_{Jmax}\,]$ or $P(T_J) = [\,T_{Jmin} \quad T_{J0}\,]$, $^\circ C$		Measured Mix Temperature $P(T_T) = [\,T_{T0} \quad T_{Tmax}\,]$ or $P(T_T) = [\,T_{Tmin} \quad T_{T0}\,]$, $^\circ C$		Measured Volume $P(V_T) = [\,V_{T0} \quad V_{Tmax}\,]$ or $P(V_T) = [\,V_{Tmin} \quad V_{T0}\,]$, m^3	
Anomaly	Pattern	Size	Pattern	Size	Pattern	Size
2nd	+	[104.1092 110.1360]	−	[29.8881 33.5265]	+	[180.3020 196.1848]
3rd	+	[104.1092 111.0231]	−	[31.7965 33.5265]	0	[180.2768 180.3020]
5th	−	[89.1025 104.1092]	−	[30.3771 33.5265]	0	[180.3020 180.5776]
7th	+	[104.1092 111.5119]	−−	[28.1455 33.5265]	0	[180.3020 180.7830]
8th	−	[97.2710 104.1092]	0	[33.5265 33.6023]	−	[162.0445 180.3020]
10th	−	[101.0274 104.1092]	0	[32.8348 33.5265]	0	[180.3020 180.3476]

Table 5.3: Fault Isolation Stage 1 in the Nominal Case

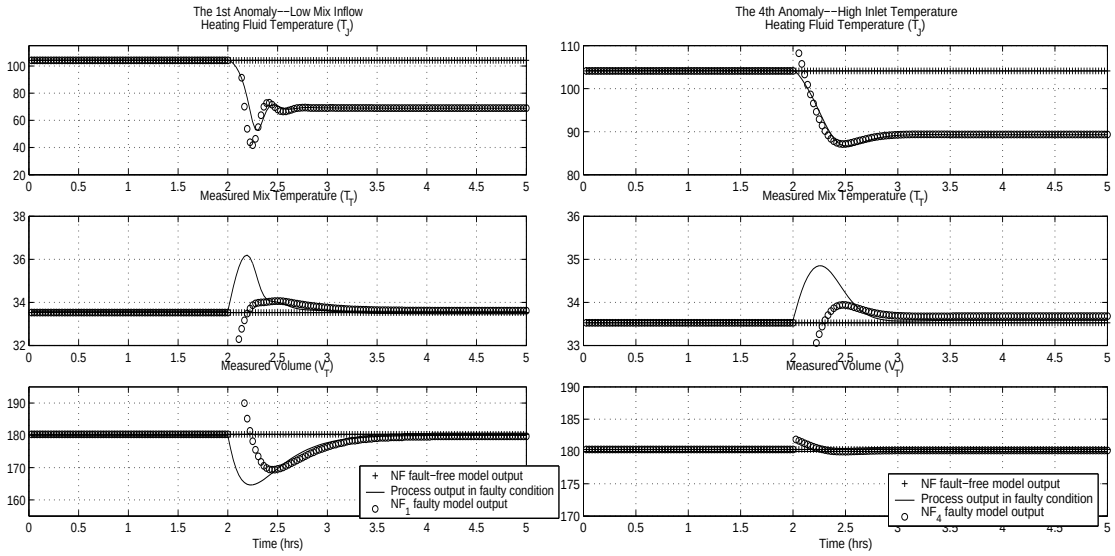

(a) Anomaly 1 (b) Anomaly 4

Figure 5.8: Anomaly Isolation Stage 2 in the Nominal Case

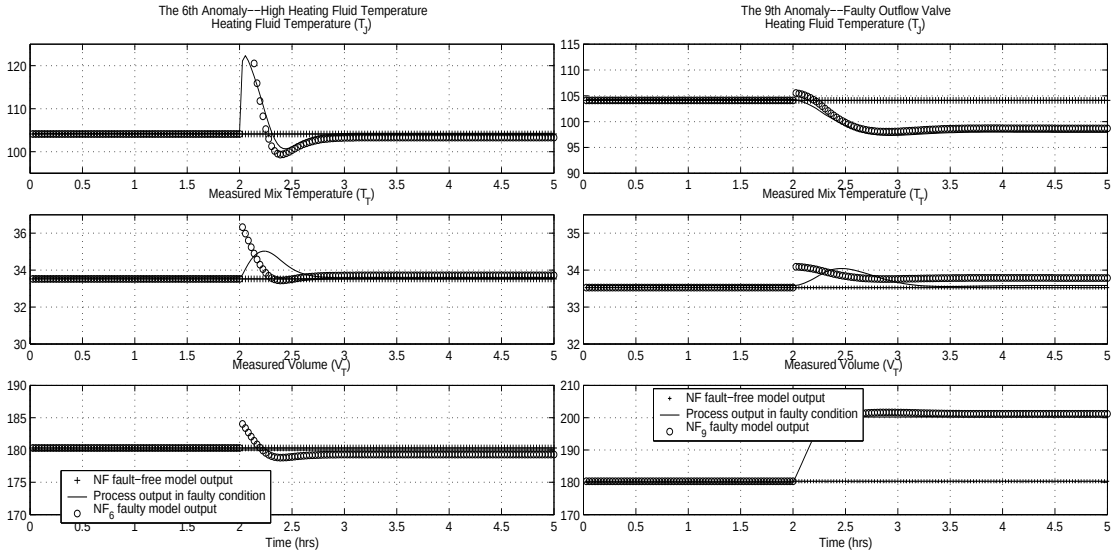

(a) Anomaly 6 (b) Anomaly 9

Figure 5.9: Anomaly Isolation Stage 2 in the Nominal Case

Fault Isolation, Stage 2						
	Heating Fluid Temperature $P(T_J) = [\,T_{J0} \quad T_{Jmax}\,]$ or $P(T_J) = [\,T_{Jmin} \quad T_{J0}\,]$, $^\circ C$		Measured Mix Temperature $P(T_T) = [\,T_{T0} \quad T_{Tmax}\,]$ or $P(T_T) = [\,T_{Tmin} \quad T_{T0}\,]$, $^\circ C$		Measured Volume $P(V_T) = [\,V_{T0} \quad V_{Tmax}\,]$ or $P(V_T) = [\,V_{Tmin} \quad V_{T0}\,]$, m^3	
Anomaly	Pattern	Size	Pattern	Size	Pattern	Size
1st	$---$	[66.5292 104.1092]	0	[33.5265 34.0617]	$-\Rightarrow 0$	[169.5783 180.3020]
4th	$-$	[87.1606 104.1092]	0	[33.5265 33.9386]	0	[180.1590 180.3020]
6th	$-\Rightarrow 0$	[100.3641 104.1092]	0	[33.5265 33.7141]	0	[179.3016 180.3020]
9th	$-$	[98.0391 104.1092]	0	[33.5265 33.8371]	$++$	[180.3020 201.6231]

Table 5.4: Fault Isolation Stage 2 in the Nominal Case

3 Summary

The above two isolation stages in the nominal case are shown in Table 5.5. The ♡ indicates the isolated anomalies. So all the anomalies can be isolated 30 minutes after they occur.

Fault Isolation Stages		
Anomaly	From Hour 2.1 - Stage 1	From Hour 2.5 - Stage 2
1st		♡
2nd	♡	♡
3rd	♡	♡
4th		♡
5th	♡	♡
6th		♡
7th	♡	♡
8th	♡	♡
9th		♡
10th	♡	♡

Table 5.5: Fault Isolation Stages in the Nominal Case

5.5.3 Ten Percent Offset of the Neuro-Fuzzy Model

In this section, the operating point of the measured volume is decreased 10 percent ($dV_{sp} = -18\,m^3$), the measured mix temperature is also decreased 10 percent ($dT_{sp} = -3.35\,°C$), and we use the same Neuro-Fuzzy models to diagnose anomalies under this level of offset.

1 Fault Detection Stage

All ten anomalies are displayed in the figures and tables that follow. Two of these anomalies are discussed as examples to illustrate the detection stage, and the other anomalies are attached in Appendix B. From the results, all the single anomalies can be detected. In Figure 5.10, the *plus* variables indicate the NF model outputs under normal conditions, and the *star* variables indicate the system process outputs in faulty conditions.

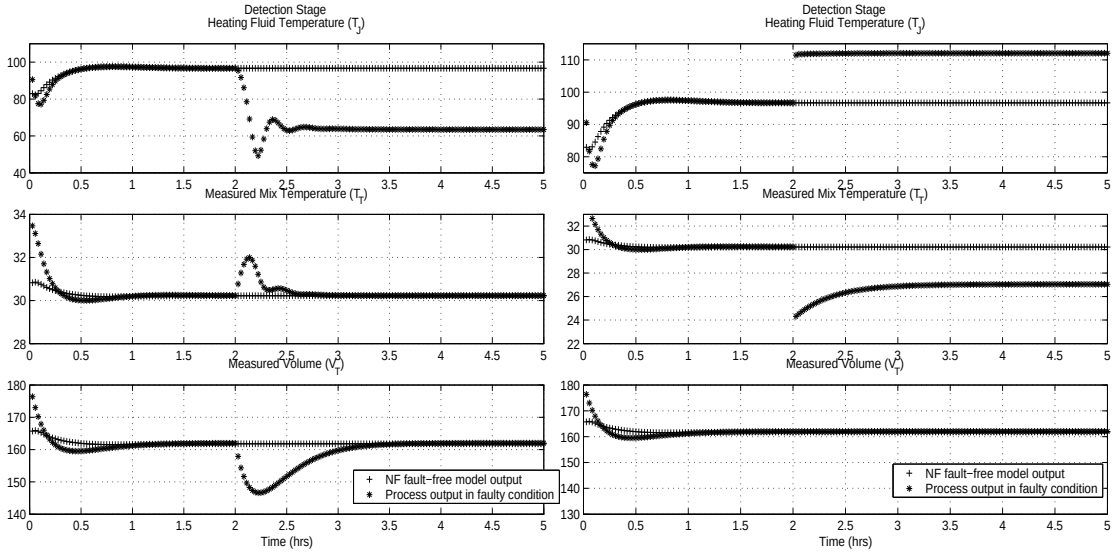

(a) Anomaly 1 (b) Anomaly 7

Figure 5.10: Anomaly Detection at Ten Percent Offset

Figure 5.10 (a) shows the effect of a low mix inflow disturbance faulty behavior which decreases by 50 percent at hour 2. The heating fluid temperature decreases by 36 percent, the measured mix temperature increases by 6 percent and returns to normal condition, and the measured volume decreases by 10 percent and then get back to normal. Thus all of the three output variables have changes.

Figure 5.10 (b) shows faulty behavior of a faulty temperature sensor which decreases by 20 percent at hour 2. The heating fluid temperature increases by 15 percent, the measured mix temperature decreases by 21 percent, and the measured volume has no change. Two of the output variables have changes.

In the detection stage, from hour 0 to hour 2, the Neuro-Fuzzy model is in the normal condition, so there is no anomaly in the system. Based on the fault-free Neuro-Fuzzy model NF_0, we detected an anomaly in the system just after hour 2. The other results are attached in Appendix B.

2 Fault Isolation Stage

In the isolation stage, from hour 2 to hour 5, we use the same bank of Neuro-Fuzzy faulty models NF_1 to NF_{10} (which are developed offine) to isolate each of the ten anomalies.

In Figure 5.11 to Figure Figure 5.16, the *plus* variables indicate the NF model outputs in normal conditions, the *circle* variables indicate the NF model outputs in faulty conditions, and the *solid* variables indicate the system process outputs in faulty conditions. The *solid* variables are used to determine whether NF faulty models have good performance. Table 5.6 and Table 5.7 show the results of the isolation stages using the Neuro-Fuzzy models. For the three output variables, as before, each variable has a pair of values which constitute the "symptoms" used for isolation, as discussed below.

For the heating fluid temperature, $T_{J0} = 96.6733\,^{\circ}C$ is the value in normal conditions, and other values of $P(T_J)$ are recorded, namely the minimum (T_{Jmin})

or maximum (T_{Jmax}) values in the faulty condition. The determination of the threshold in normal condition, the determination of the range of different degrees, and the determination of different patterns are the same as the nominal case.

For the measured mix temperature, $T_{T0} = 30.2185\,°C$ is the value in normal conditions, and other values of $P(T_T)$ are recorded, namely the minimum (T_{Tmin}) or maximum (T_{Tmax}) value in the faulty condition. The determination of the threshold in normal condition, the determination of the range of different degrees, and the determination of different patterns are the same as the nominal case.

For the measured volume, $V_{T0} = 161.7959\,m^3$ is the value in normal condition, and other values of $P(V_T)$ are recorded, namely the minimum (V_{Tmin}) or maximum (V_{Tmax}) value in the faulty condition. The determination of the threshold in normal condition, the determination of the range of different degrees, and the determination of the different patterns are the same as the nominal case.

Thus, in Table 5.6 to Table 5.7, those patterns are denoted by '0', '$-$', '$---$', '$+$', '$+++$', '$+\Rightarrow 0$', and '$-\Rightarrow 0$' based on the behavior of '*unchanged*', '*decreases to low degree*', '*decreases to very very low degree*', '*increases to high degree*', '*increases to very very high degree*', '*decreases from high degree to normal condition*', and '*increases from low degree to normal condition*' symptoms.

Figure 5.11 to Figure 5.13 and Table 5.6 illustrate the first isolation stage. From

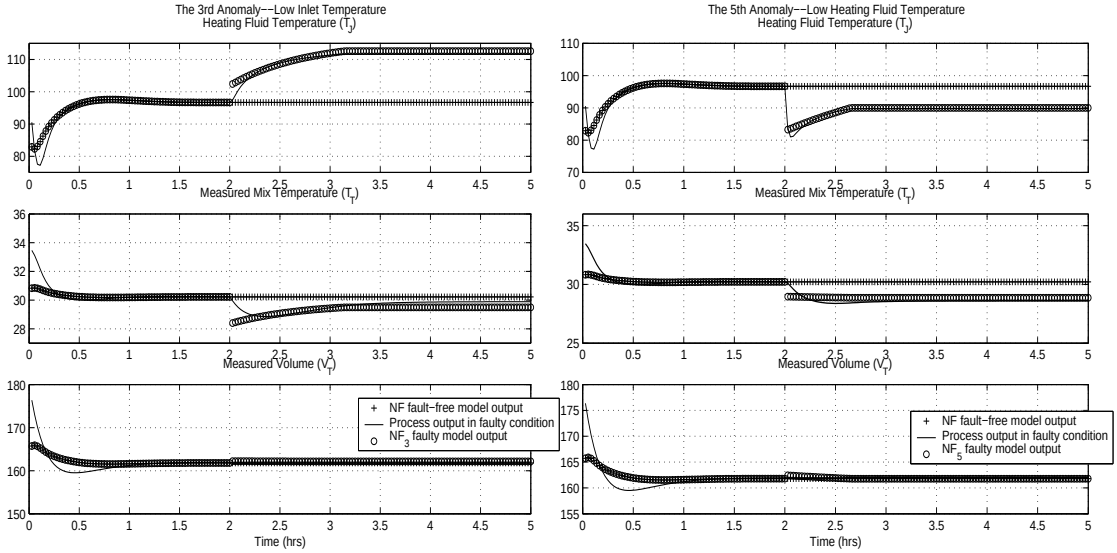

(a) Anomaly 3 (b) Anomaly 5

Figure 5.11: Anomaly Isolation Stage 1 at Ten Percent Offset

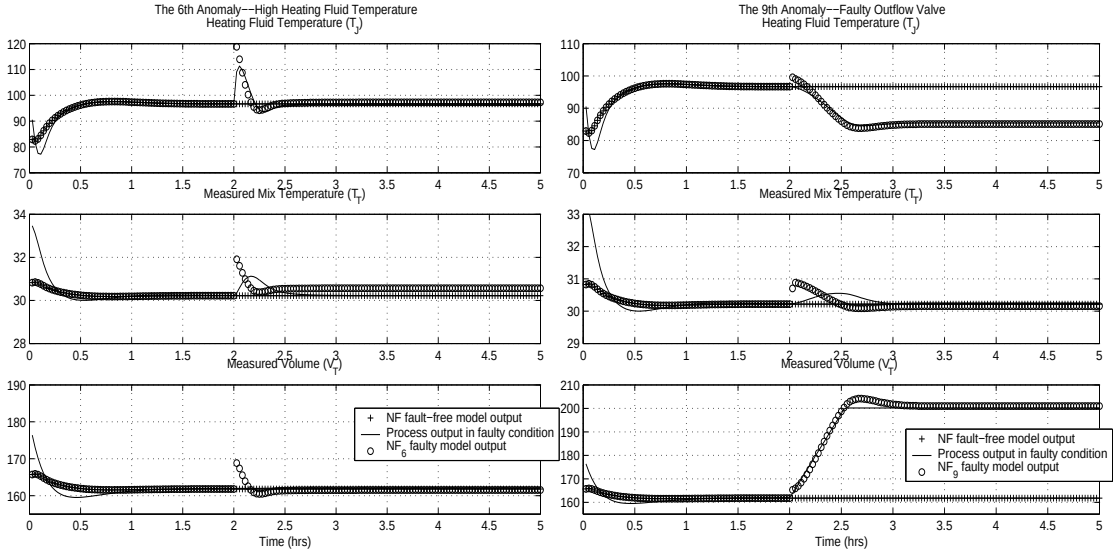

(a) Anomaly 6 (b) Anomaly 9

Figure 5.12: Anomaly Isolation Stage 1 at Ten Percent Offset

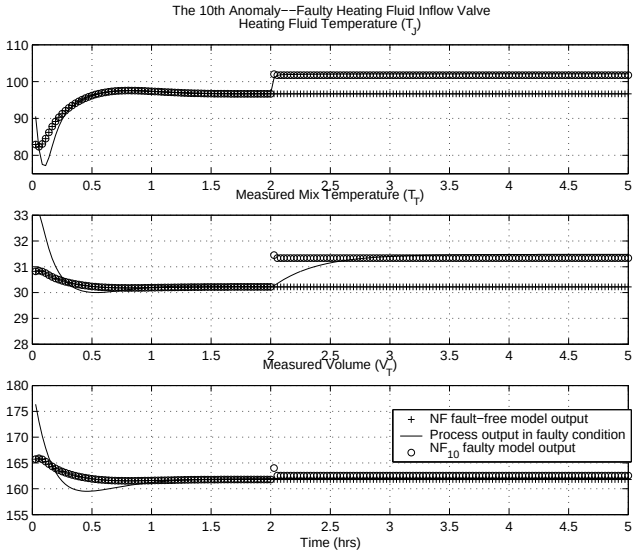

Figure 5.13: The 10th Anomaly, Isolation Stage 1 at Ten Percent Offset

hour 2.1, the three output variables of different anomalies have different patterns and sizes. We can isolate the 3rd, 5th, 6th, 9th, and 10th anomalies soon after they occur.

Fault Isolation, Stage 1						
	Heating Fluid Temperature $P(T_J) = [\,T_{J0} \quad T_{Jmax}\,]$ or $P(T_J) = [\,T_{Jmin} \quad T_{J0}\,]$, $^\circ C$		Measured Mix Temperature $P(T_T) = [\,T_{T0} \quad T_{Tmax}\,]$ or $P(T_T) = [\,T_{Tmin} \quad T_{T0}\,]$, $^\circ C$		Measured Volume $P(V_T) = [\,V_{T0} \quad V_{Tmax}\,]$ or $P(V_T) = [\,V_{Tmin} \quad V_{T0}\,]$, m^3	
Anomaly	Pattern	Size	Pattern	Size	Pattern	Size
3rd	+	[96.6733 112.5615]	$-\Rightarrow 0$	[28.6010 30.2185]	0	[161.7959 162.1454]
5th	−	[84.5856 96.6733]	−	[28.8635 30.2185]	0	[161.7724 161.7959]
6th	$+\Rightarrow 0$	[96.6733 100.2204]	0	[30.2185 30.7516]	0	[161.7959 162.5652]
9th	−	[83.8178 96.6733]	0	[30.2185 30.7991]	+ + +	[161.7959 204.1402]
10th	+	[96.6733 101.7396]	+	[30.2185 31.3336]	0	[161.7959 162.5476]

Table 5.6: Fault Isolation Stage 1 at Ten Percent Offset

Figure 5.14 to Figure 5.16 and Table 5.7 illustrate the second isolation stage. From hour 2.5, the three output variables of different anomalies have different patterns and sizes. We can isolate the 1st, 2nd, 4th, 7th, and 8th anomalies

within 30 minutes.

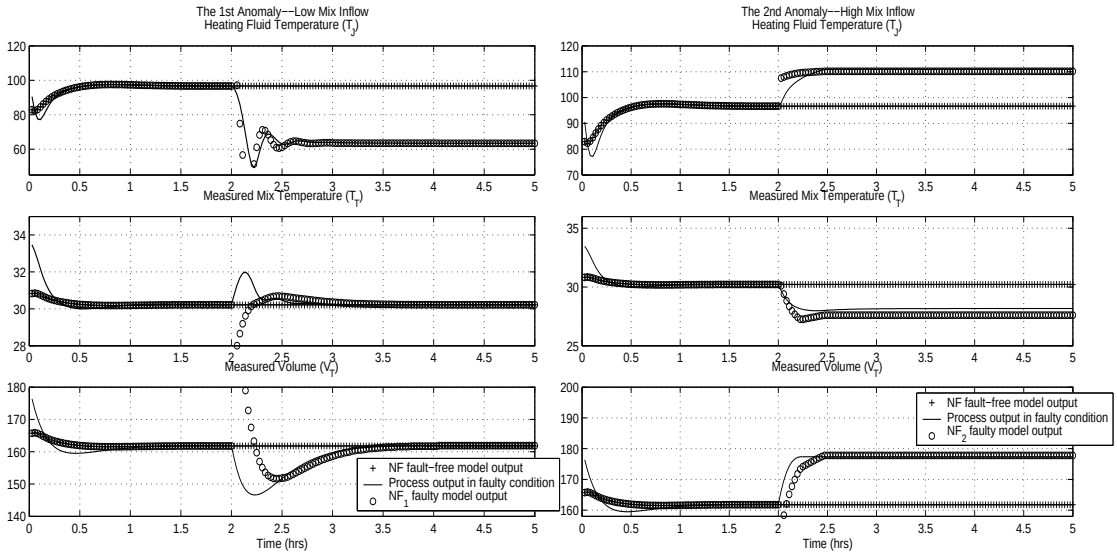

(a) Anomaly 1 (b) Anomaly 2

Figure 5.14: Anomaly Isolation Stage 2 at Ten Percent Offset

Fault Isolation, Stage 2						
	Heating Fluid Temperature $P(T_J) = [\,T_{J0} \quad T_{Jmax}\,]$ or $P(T_J) = [\,T_{Jmin} \quad T_{J0}\,]$, $^\circ C$		Measured Mix Temperature $P(T_T) = [\,T_{T0} \quad T_{Tmax}\,]$ or $P(T_T) = [\,T_{Tmin} \quad T_{T0}\,]$, $^\circ C$		Measured Volume $P(V_T) = [\,V_{T0} \quad V_{Tmax}\,]$ or $P(V_T) = [\,V_{Tmin} \quad V_{T0}\,]$, m^3	
Anomaly	Pattern	Size	Pattern	Size	Pattern	Size
1st	$- - -$	[61.0641 96.6733]	0	[30.2185 30.6767]	$-\Rightarrow 0$	[151.8216 161.7959]
2nd	$+$	[96.6733 110.1360]	$-$	[27.5978 30.2185]	$+$	[161.7959 177.8241]
4th	$-$	[80.3966 96.6733]	0	[30.2185 30.4359]	0	[161.7959 162.1668]
7th	$+$	[96.6733 112.0293]	$-$	[26.7357 30.2185]	0	[161.7959 162.0533]
8th	$-$	[84.7866 96.6733]	0	[30.0791 30.2185]	0	[159.0385 161.7959]

Table 5.7: Fault Isolation Stage 2 at Ten Percent Offset

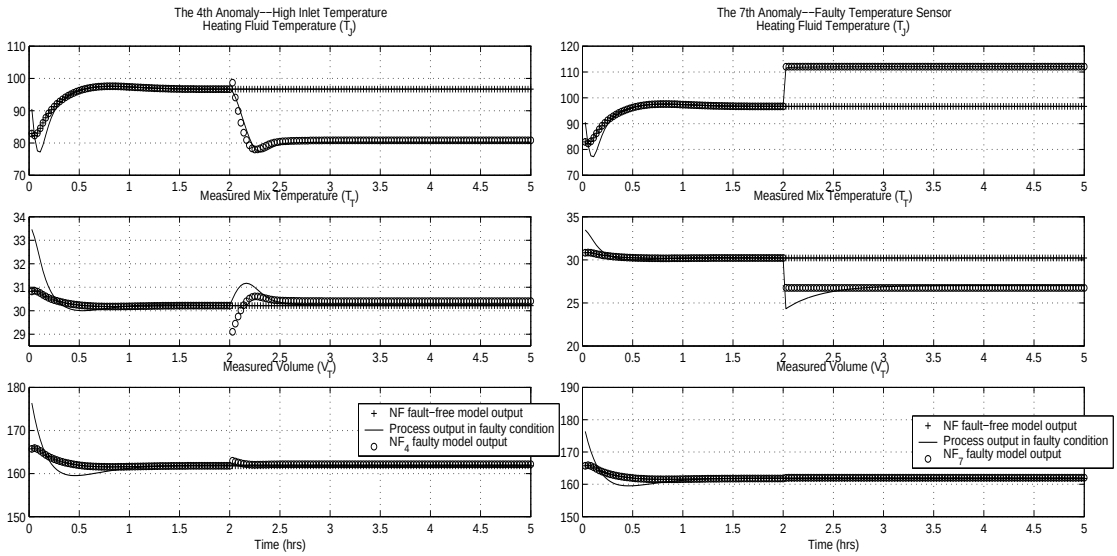

(a) Anomaly 4 (b) Anomaly 7

Figure 5.15: Anomaly Isolation Stage 2 at Ten Percent Offset

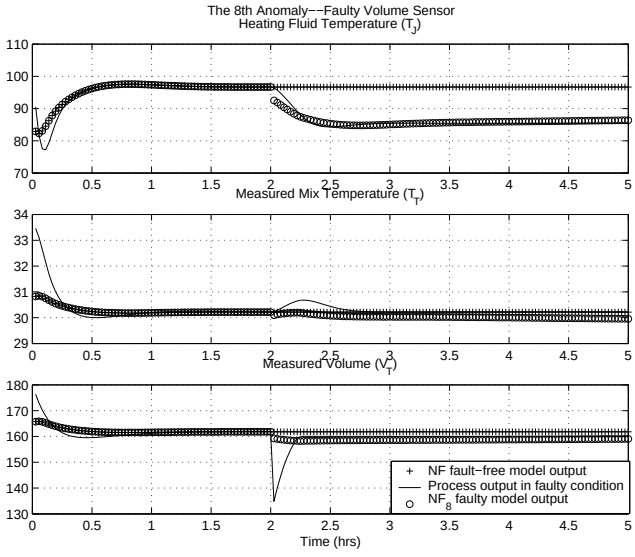

Figure 5.16: The 8th Anomaly, Isolation Stage 2 at Ten Percent Offset

3 Summary

The above two isolation stages are shown in Table 5.8. The ♡ indicates the successfully isolated anomalies. So all the anomalies can be isolated after they occur.

Fault Isolation Stages		
Anomaly	From Hour 2.1 - Stage 1	From Hour 2.5 - Stage 2
1st		♡
2nd		♡
3rd	♡	♡
4th		♡
5th	♡	♡
6th	♡	♡
7th		♡
8th		♡
9th	♡	♡
10th	♡	♡

Table 5.8: Fault Isolation Stages at Ten Percent Offset

5.5.4 Thirty Percent Offset of the Neuro-Fuzzy Model

In this study, when the operating points of the measured volume and the measured mix temperature are both decreased 30 percent ($dV_{sp} = -54\,m^3, dT_{sp} = -10\,^\circ C$), we use the same Neuro-Fuzzy models to diagnose anomalies under this level of offset. We obtain the following results; note that the procedure is identical to the previous discussions, so it is only briefly outlined here.

1 Fault Detection Stage

The same two anomalies are presented in Figure 5.17. Again, detection is successful for each anomaly.

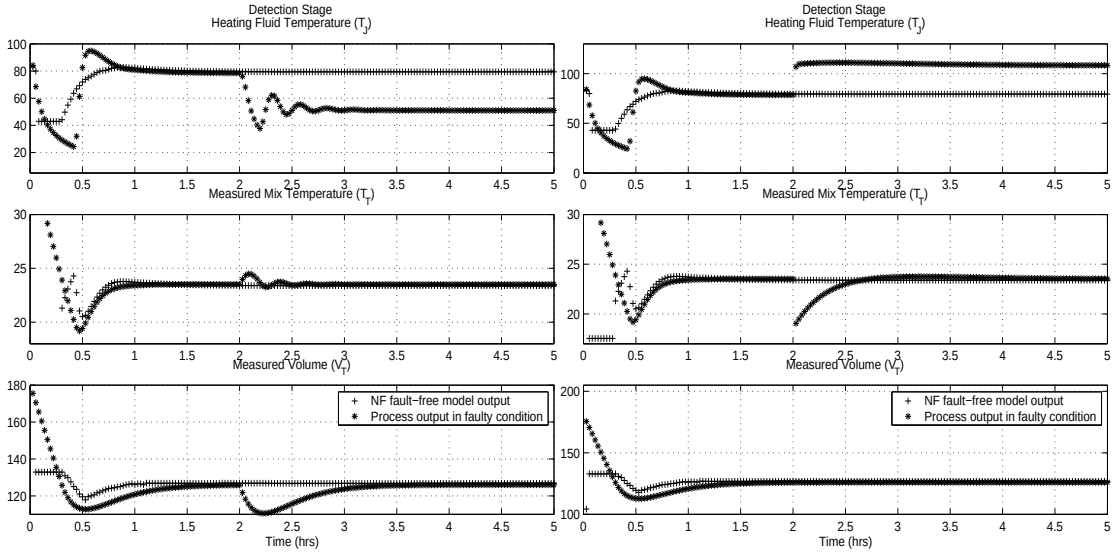

(a) Anomaly 1 (b) Anomaly 7

Figure 5.17: Anomaly Detection Stage at Thirty Percent Offset

2 Fault Isolation Stage

As before, at hour 2 to hour 5, we switch to the same bank of Neuro-Fuzzy faulty models (NF_1 to NF_{10}) to isolate the anomalies. Table 5.9 illustrates the first isolation stage. From hour 2.1, we can isolate the 2nd, 3rd, 5th, and 8th anomalies soon after they occur. Table 5.10 illustrates the second isolation stage. From hour 2.5, we can isolate the 4th, 6th, 7th, and 10th anomalies within 30 minutes. Table 5.11 illustrates the third isolation stage. From hour 3, we can isolate the 1st and 9th anomalies within one hour after they occur. At this time all anomalies are successfully isolated.

Fault Isolation, Stage 1						
	Heating Fluid Temperature $P(T_J) = [\,T_{J0} \quad T_{Jmax}\,]$ or $P(T_J) = [\,T_{Jmin} \quad T_{J0}\,]$, $^\circ C$		Measured Mix Temperature $P(T_T) = [\,T_{T0} \quad T_{Tmax}\,]$ or $P(T_T) = [\,T_{Tmin} \quad T_{T0}\,]$, $^\circ C$		Measured Volume $P(V_T) = [\,V_{T0} \quad V_{Tmax}\,]$ or $P(V_T) = [\,V_{Tmin} \quad V_{T0}\,]$, m^3	
Anomaly	Pattern	Size	Pattern	Size	Pattern	Size
2nd	++	[79.4174 99.2282]	0	[23.3031 23.3934]	+	[126.8561 141.2388]
3rd	++	[79.4174 100.1229]	0	[23.1282 23.3934]	0	[126.1383 126.8561]
5th	$-\Rightarrow 0$	[72.748 79.4174]	0	[23.3934 24.0187]	0	[126.5575 126.8561]
8th	−	[69.3263 79.4174]	0	[23.2022 23.3934]	$-\Rightarrow 0$	[119.1147 126.5575]

Table 5.9: Fault Isolation Stage 1 at Thirty Percent Offset

Fault Isolation, Stage 2						
	Heating Fluid Temperature $P(T_J) = [\,T_{J0} \quad T_{Jmax}\,]$ or $P(T_J) = [\,T_{Jmin} \quad T_{J0}\,]$, $^\circ C$		Measured Mix Temperature $P(T_T) = [\,T_{T0} \quad T_{Tmax}\,]$ or $P(T_T) = [\,T_{Tmin} \quad T_{T0}\,]$, $^\circ C$		Measured Volume $P(V_T) = [\,V_{T0} \quad V_{Tmax}\,]$ or $P(V_T) = [\,V_{Tmin} \quad V_{T0}\,]$, m^3	
Anomaly	Pattern	Size	Pattern	Size	Pattern	Size
4st	−−	[58.3150 79.4174]	0	[23.1692 23.3934]	0	[126.3843 126.8561]
6th	0	[78.0660 79.4174]	0	[23.3934 23.5368]	0	[125.8870 126.8561]
7th	++	[79.4174 111.2284]	0	[23.3934 24.0695]	0	[126.0907 126.8561]
10th	++	[79.4174 104.6838]	++	[23.3934 28.7420]	0	[126.4515 126.8561]

Table 5.10: Fault Isolation Stage 2 at Thirty Percent Offset

Fault Isolation, Stage 3						
	Heating Fluid Temperature $P(T_J) = [\,T_{J0} \quad T_{Jmax}\,]$ or $P(T_J) = [\,T_{Jmin} \quad T_{J0}\,]$, $^\circ C$		Measured Mix Temperature $P(T_T) = [\,T_{T0} \quad T_{Tmax}\,]$ or $P(T_T) = [\,T_{Tmin} \quad T_{T0}\,]$, $^\circ C$		Measured Volume $P(V_T) = [\,V_{T0} \quad V_{Tmax}\,]$ or $P(V_T) = [\,V_{Tmin} \quad V_{T0}\,]$, m^3	
Anomaly	Pattern	Size	Pattern	Size	Pattern	Size
1st	−−	[51.3361 79.4174]	0	[23.4659 23.3934]	0	[124.6005 126.8561]
9th	−−	[59.4132 79.4174]	0	[23.4245 23.3934]	+++++	[126.8561 206.4055]

Table 5.11: Fault Isolation Stage 3 at Thirty Percent Offset

3 Summary

The above three isolation stages are shown in Table 5.12. The ♡ indicates the successfully isolated anomalies. The figures are attached in Appendix B.

Fault Isolation Stages			
Anomaly	From Hour 2.1 - Stage 1	From Hour 2.5 - Stage 2	From Hour 3.0 - Stage 3
1st			♡
2nd	♡	♡	♡
3rd	♡	♡	♡
4th		♡	♡
5th	♡	♡	♡
6th		♡	♡
7th		♡	♡
8th	♡	♡	♡
9th			♡
10th		♡	♡

Table 5.12: Fault Isolation Stages at Thirty Percent Offset

Chapter 6

Sequential Fault Diagnosis in the JCSTR System

Here, we consider situations when two anomalies occur sequentially. At hour t_1, the first anomaly occurs, and some time later, at hour t_2, the second anomaly occurs. The set point of the measured volume is $dV_{sp} = -18\,m^3$, and the set point of the measured mix temperature is $dT_{sp} = -3.35\,^{\circ}C$. We use Neuro-Fuzzy models to detect the time of these two anomalies, and also isolate both of these two anomalies after they occur. Note that -10 percent set points were used here, again to check robustness.

6.1 Detection of Sequential Faults

In Figure 6.1, the *plus* variables indicate the Neuro-Fuzzy Model in normal conditions and the *star* variables indicate the process in faulty conditions. In the following two examples, at hour 2, the first anomaly occurs, and at hour 3.5, the second anomaly occurs in sequence.

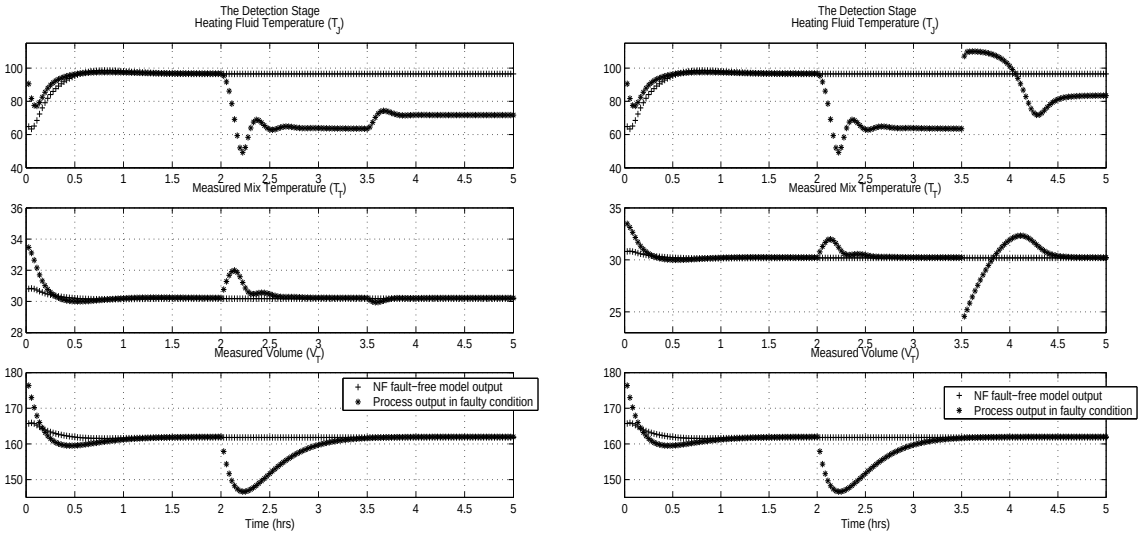

(a) Anomalies F_1 Then F_3 (b) Anomalies F_1 Then F_7

Figure 6.1: The Detection Stage Case

Figure 6.1 (a) shows that two anomalies occur sequentially. The first anomaly is the low mix inflow disturbance which occurs at hour 2. The second anomaly is the low inlet temperature disturbance, which occurs at hour 3.5. The initial transients are caused by the -10 percent set point change at t=0, and are thus ignored.

1. After hour 2, the first output, heating fluid temperature, decreases below the normal condition. After hour 3.5, the first output increases a little, due to the second anomaly, but it is still below the normal condition.

2. After hour 2, the second output, measured mix temperature, increases a little above the normal condition and returns to normal condition. After hour 3.5, there is a small transient; it seems the second anomaly has very little effect on the state of the measured mix temperature variable.

3. After hour 2, the third output, measured volume, decreases below the normal condition and then gradually returns to normal condition. After hour 3.5, the third output stays normal. It is not affected by the second anomaly, since an

inlet temperature disturbance does not excite the volume dynamics.

In Figure 6.1 (b), the first anomaly is the low mix inflow disturbance, which occurs at hour 2, and the second anomaly is the faulty temperature sensor, which occurs at hour 3.5.

1. At hour 2, the first output, heating fluid temperature, decreases below the normal condition. At hour 3.5, the first output suddenly increases greatly and rises above the normal condition, due to the second anomaly, and then gradually decreases below the normal condition again.

2. At hour 2, the second output, measured mix temperature increases a little, decreases again, and quickly returns to normal condition. At hour 3.5, the second output suddenly decreases far below the normal condition, increases above normal and then returns to normal. It seems the second anomaly affects this variable significantly.

3. At hour 2, the third output, measured volume, decreases below normal condition and then gradually returns to normal condition. At hour 3.5, the third output stays normal. The second anomaly does not affect this variable.

In the detection stage, from hour 0 to hour 2, the process and Neuro-Fuzzy model are in normal condition, so there is no anomaly in the system. Based on the fault-free Neuro-Fuzzy model NF_0, we detected the first anomaly just after hour 2, then after hour 3.5, another anomaly is detected. The next step after hour 2 is to start monitoring $NF_1 - NF_{10}$ models to perform the isolation stage, and prepare to detect and isolate the second anomaly at hour 3.5. Other results are attached in Appendix C.

6.2 Isolation of Sequential Faults

In this section, we will see how the Neuro-Fuzzy model can isolate the sequential faults after they occur. In Figure 6.2, the *plus* variables indicate the NF model output in normal conditions NF_0, the *circle* variables indicate the appropriate Neuro-Fuzzy model outputs of sequential faults (NF_k or $NF_{k,j}$, please see below) and the *solid* variables indicate the system process outputs in faulty conditions. The *solid* variables are used to determine whether NF faulty models have good performance. The first anomaly occurs at hour 2, the second anomaly occurs at hour 3.5.

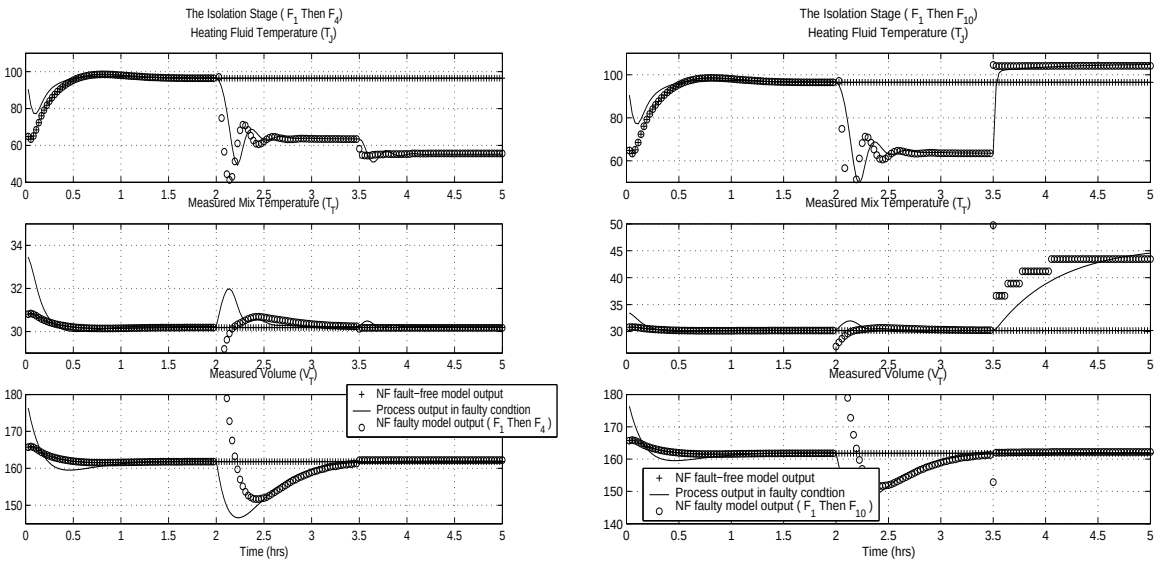

(a) Anomalies F_1 Then F_4 (b) Anomalies F_1 Then F_{10}

Figure 6.2: Sequential Faults Isolation Stage

From hour 2 (just after detection), we switch to the first bank of NF faulty models $NF_k,\ k = 1, 2, ..., 10$, in order to isolate the first anomaly and detect the second one. From hour 3.5 (just after the second detection), we switch to a second bank of NF faulty models $NF_{k,j},\ j = 1, 2, ..., 10$, where the index k is determined by the first anomaly isolated. We use these Neuro-Fuzzy models to isolate the second fault. Table 6.1 and Table 6.2 show the isolation stages of the sequential faults, using the

Neuro-Fuzzy models. For the three output variables, each variable is defined by two values, and corresponding patterns are denoted by '0', '$-$', '$--$', '$+$', etc., as before.

Sequential Fault Isolation Stage, F_1 Then F_4						
	Heating Fluid Temperature $P(T_J) = [\,T_{J0} \quad T_{Jmax}\,]$ or $P(T_J) = [\,T_{Jmin} \quad T_{J0}\,]$, $^\circ C$		Measured Mix Temperature $P(T_T) = [\,T_{T0} \quad T_{Tmax}\,]$ or $P(T_T) = [\,T_{Tmin} \quad T_{T0}\,]$, $^\circ C$		Measured Volume $P(V_T) = [\,V_{T0} \quad V_{Tmax}\,]$ or $P(V_T) = [\,V_{Tmin} \quad V_{T0}\,]$, m^3	
Anomaly	Pattern	Size	Pattern	Size	Pattern	Size
1st	$--$	[61.0641 96.6733]	0	[30.2185 30.6767]	$-\Rightarrow 0$	[151.8216 161.7959]
4th	$---$	[54.4783 96.6733]	0	[30.1683 30.2185]	0	[161.7959 162.2172]

Table 6.1: Sequential Faults Isolation Stage, F_1 Then F_4

Sequential Fault Isolation Stage, F_1 Then F_{10}						
	Heating Fluid Temperature $P(T_J) = [\,T_{J0} \quad T_{Jmax}\,]$ or $P(T_J) = [\,T_{Jmin} \quad T_{J0}\,]$, $^\circ C$		Measured Mix Temperature $P(T_T) = [\,T_{T0} \quad T_{Tmax}\,]$ or $P(T_T) = [\,T_{Tmin} \quad T_{T0}\,]$, $^\circ C$		Measured Volume $P(V_T) = [\,V_{T0} \quad V_{Tmax}\,]$ or $P(V_T) = [\,V_{Tmin} \quad V_{T0}\,]$, m^3	
Anomaly	Pattern	Size	Pattern	Size	Pattern	Size
1st	$--$	[61.0641 96.6733]	0	[30.2185 30.6767]	$-\Rightarrow 0$	[151.8216 161.7959]
10th	$+$	[96.6733 104.1228]	$+++$	[30.2185 43.4662]	0	[161.7959 162.2112]

Table 6.2: Sequential Faults Isolation Stage, F_1 Then F_{10}

For the sequential anomalies in Figure 6.2 (a), the first anomaly is isolated at hour 2.5 (after large transients have decayed): the heating fluid temperature decreases, the measured mix temperature increases and returns to normal, and the measured volume decreases and then returns to normal condition. Table 6.1 shows the patterns and sizes of the three outputs for the first anomaly. This anomaly is low mix inflow disturbance, the first anomaly of the ten anomalies. At this time we monitor the model NF_1 to detect any further faults that might occur. Immediately after hour 3.5 the second fault is detected and we switch to the bank of NF models $NF_{1,1}$, $NF_{1,2}$, ..., $NF_{1,10}$.

At hour 3.6, Figure 6.2 (a) shows that the three output variables begin to change due to the second anomaly. The heating fluid temperature decreases again, the measured mix temperature does not change, and the measured volume does not change. Table 6.2 shows the pattern and size of the second anomaly, which matches the pattern of model $NF_{1,4}$, so we isolate the anomaly as high inlet temperature disturbance, the fourth anomaly of the ten anomalies. The patterns and sizes of the other $NF_{1,j}$ models, $j \neq 4$ do not match, so the isolation is clear. These two anomalies have different patterns and sizes, so we can isolate this sequential faults after they occur.

For the sequential anomalies in Figure 6.2 (b), the first anomaly is isolated at hour 2.5: the heating fluid temperature decreases, the measured mix temperature increases and quickly returns to normal, and the measured volume decreases and then returns to normal condition. Table 6.2 shows the pattern and size of the first anomaly. This anomaly is low mix inflow disturbance, the first anomaly of the ten anomalies. Again, at this time we monitor the model NF_1 to detect any further faults that might occur.

At hour 3.6, Figure 6.2 (b) shows that the three output variables begin to change due to the second anomaly. The heating fluid temperature increases above the normal condition, the measured mix temperature increases gradually above the normal condition, and the measured volume does not change. Table 6.2 shows the pattern and size of the second anomaly, which matches the pattern of model $NF_{1,10}$, so we isolate the anomaly as faulty heating fluid inflow valve fault, the tenth anomaly. These two anomalies have different patterns and sizes, so we can isolate these sequential faults after they occur. Some other results are included in Appendix C.

Chapter 7

Neuro-Fuzzy Identification for Arbitrary Fault Size

7.1 Introduction

There are 10 different anomalies considered previously of known size. Low mix inflow and high mix inflow disturbances are the same type of anomaly, although they have different signs, we combine them into one anomaly, *F*1*: Mix Inflow Disturbance*. Low inlet temperature and high inlet temperature disturbances can be combined as *F*2*: Inlet Temperature Disturbance*, and low heating fluid temperature and high heating fluid temperature can be combined as *F*3*: Heating Fluid Temperature Disturbance*. The other four anomalies are unchanged, so there are seven anomalies listed in the following:

1. *F*1*: Mix Inflow Disturbance*
2. *F*2*: Inlet Temperature Disturbance*
3. *F*3*: Heating Fluid Temperature Disturbance*
4. *F*4*: Faulty Temperature Sensor Fault*

5. *F5: Faulty Volume Sensor Fault*

6. *F6: Faulty Outflow Valve Fault*

7. *F7: Faulty Heating Fluid Inflow Valve Fault.*

In previous chapters, we considered anomalies of specific known size. Here we show how to deal with anomalies of unknown magnitude. We use the Neuro-Fuzzy model to generate symptoms that can be used to identify the seven anomalies by applying different fault size changes. We consider ten fault size cases: ± 0.2, ± 0.4, ± 0.6, ± 0.8, and ± 1.0. Each anomaly is applied with those 10 fault sizes, and we use the NF model to produce their symptoms. This creates a mapping of symptom size versus anomaly size that can be used with a pattern matching algorithm to solve the isolation problem for arbitrary anomaly sizes.

7.1.1 Identifying the Faults

In Figure 7.1, the *star* variables indicate the symptoms of *F2: Inlet Temperature Disturbance*, the *circle* variables indicate the symptom of *F7: Faulty Heating Fluid Inflow Valve Fault*, and the *plus* variables indicate the NF model in normal condition. The values plotted show the deviations caused by anomalies ranging from -100 percent to 100 percent in the three outputs monitored for symptom evaluation. Table 7.1 shows the symptoms of $F2$ and $F7$ anomalies for ten fault size cases (these cases are combined in the figures and tables to save space). As before, each "symptom" is defined by two values.

In this Figure, the X axis indicates ten different fault sizes from -1.0 to $+1.0$, and the Y axes indicate the three output symptoms that are produced by the NF models

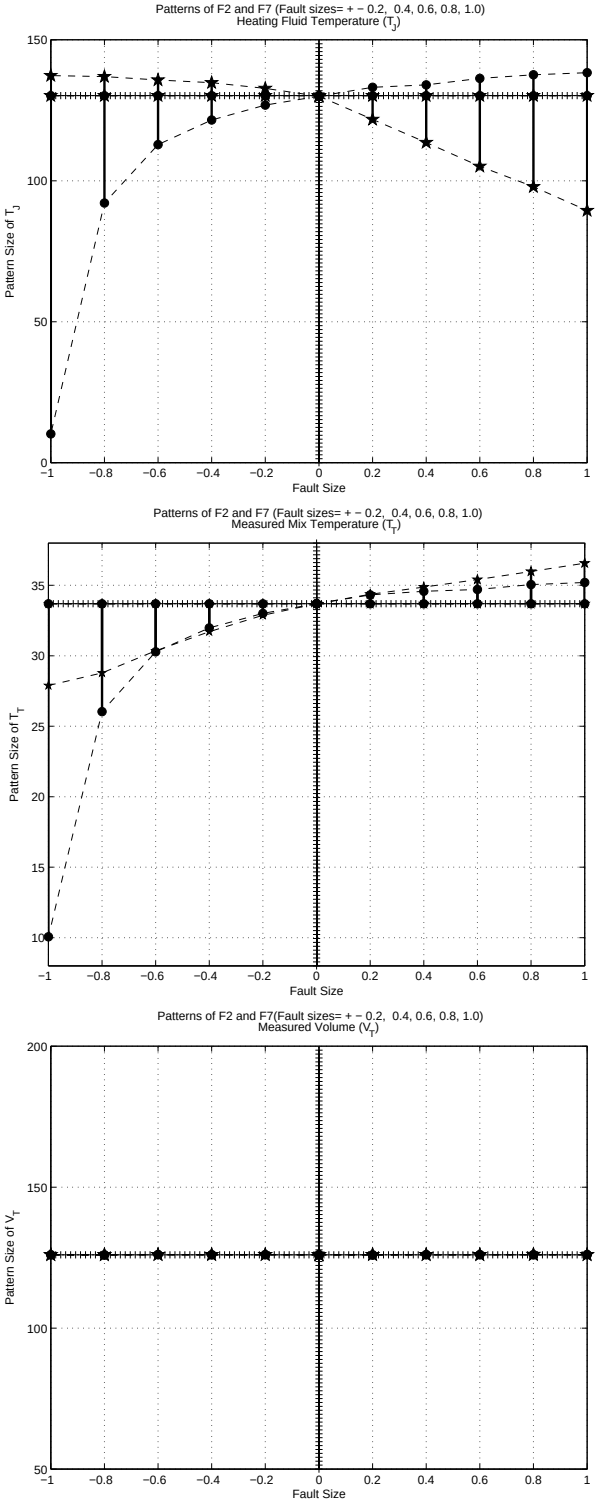

Figure 7.1: Output Variable Patterns for $F2$ and $F7$

corresponding to these ten fault size cases. As before, they are called "pattern sizes", for a range of fault sizes rather than a fixed fault size. Corresponding to each fault size, its "pattern size" is represented by three pairs of values, which are shown in Table 7.1.

For the heating fluid temperature variable, Figure 7.1(a) and Table 7.1 show its pattern sizes; $F2$ and $F7$ have different pattern sizes for all fault sizes. For the measured mix temperature variable, Figure 7.1(b) and Table 7.1 show its pattern sizes; $F2$ and $F7$ have similar pattern sizes at fault sizes ± 0.2, ± 0.4, and $+0.6$, but have different pattern sizes for other fault sizes. For the measured volume variable, Figure 7.1(c) and Table 7.1 show its pattern sizes; $F2$ and $F7$ have similar pattern sizes for all fault sizes.

These observations show that we need to consider the three output variables to isolate the two anomalies. As the heating fluid temperature has totally different pattern sizes for $F2$ and $F7$ for all fault size cases, we can isolate $F2$*: Inlet Temperature Disturbance* and $F7$*: Faulty Heating Fluid Inflow Valve Fault.* Some other results are attached in Appendix D.

Fault Isolation Stage for $F2$ and $F7$						
	Heating Fluid Temperature $P(T_J) = [\,T_{J0} \quad T_{Jmax}\,]$ or $P(T_J) = [\,T_{Jmin} \quad T_{J0}\,]$, $^\circ C$		Measured Mix Temperature $P(T_T) = [\,T_{T0} \quad T_{Tmax}\,]$ or $P(T_T) = [\,T_{Tmin} \quad T_{T0}\,]$, $^\circ C$		Measured Volume $P(V_T) = [\,V_{T0} \quad V_{Tmax}\,]$ or $P(V_T) = [\,V_{Tmin} \quad V_{T0}\,]$, m^3	
Anomaly	Fault Size	Pattern Size	Fault Size	Pattern Size	Fault Size	Pattern Size
$F2$	-0.2	[130.1909 132.7838]	-0.2	[32.8694 33.6885]	-0.2	[126.0776 126.0445]
$F2$	-0.4	[130.1909 134.7964]	-0.4	[31.7103 33.6885]	-0.4	[126.0445 126.0804]
$F2$	-0.6	[130.1909 135.7571]	-0.6	[30.3517 33.6885]	-0.6	[126.0445 126.0704]
$F2$	-0.8	[130.1909 136.9463]	-0.8	[28.7868 33.6885]	-0.8	[125.9414 126.0445]
$F2$	-1.0	[130.1909 137.3262]	-1.0	[27.8875 33.6885]	-1.0	[125.9975 126.0445]
$F2$	0.2	[121.7667 130.1909]	0.2	[33.6885 34.3623]	0.2	[126.0445 126.0513]
$F2$	0.4	[113.5679 130.1909]	0.4	[33.6885 34.8769]	0.4	[126.0178 126.0445]
$F2$	0.6	[105.1324 130.1909]	0.6	[33.6885 35.4049]	0.6	[125.9773 126.0445]
$F2$	0.8	[97.8745 130.1909]	0.8	[33.6885 35.9842]	0.8	[126.0445 126.1425]
$F2$	1.0	[89.4537 130.1909]	1.0	[33.6885 36.5718]	1.0	[125.9821 126.0445]
$F7$	-0.2	[126.8499 130.1909]	-0.2	[33.0051 33.6885]	-0.2	[126.0445 126.0611]
$F7$	-0.4	[121.5481 130.1909]	-0.4	[31.9813 33.6885]	-0.4	[126.0112 126.0445]
$F7$	-0.6	[112.8213 130.1909]	-0.6	[30.2849 33.6885]	-0.6	[126.1042 126.0445]
$F7$	-0.8	[92.0940 130.1909]	-0.8	[26.0341 33.6885]	-0.8	[125.9017 126.0445]
$F7$	-1.0	[10.2109 130.1909]	-1.0	[10.0619 33.6885]	-1.0	[125.9563 126.0445]
$F7$	0.2	[130.1909 133.1452]	0.2	[33.6885 34.3217]	0.2	[125.8826 126.0445]
$F7$	0.4	[130.1909 134.0199]	0.4	[33.6885 34.5756]	0.4	[125.9560 126.0445]
$F7$	0.6	[130.1909 136.3253]	0.6	[33.6885 34.7037]	0.6	[126.0445 126.0595]
$F7$	0.8	[130.1909 137.5921]	0.8	[33.6885 35.0510]	0.8	[126.0232 126.0445]
$F7$	1.0	[130.1909 138.3256]	1.0	[33.6885 35.1985]	1.0	[126.0445 126.0948]

Table 7.1: Fault Isolation Stage for $F2$ and $F7$

7.2 Fault Size and Type Identification

7.2.1 Objective

In this section, we assume we know the pattern sizes for the seven anomalies for 10 fault sizes, based on offline simulation. The objective is to determine the type and size of an unknown anomaly using the interpolation method.

7.2.2 Fault Size and Type Identification

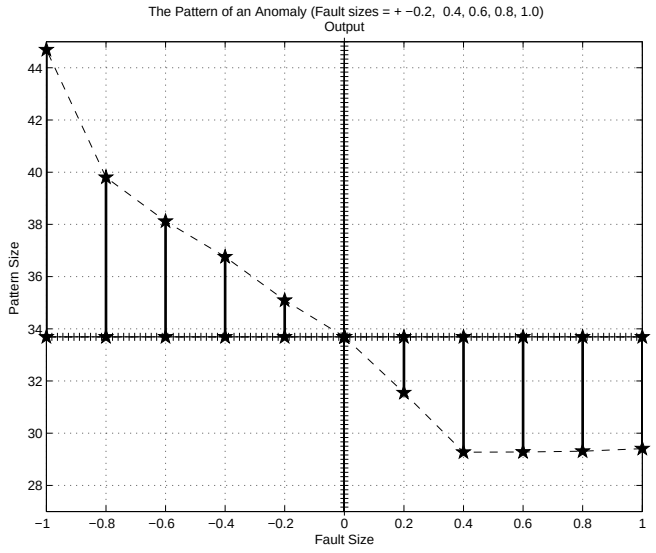

Figure 7.2: The Pattern Figure of One Symptom

1 Interpolation Stage:

As shown in Figure 7.2, from the negative side to the positive side of the X axis, there are 10 bins, each bin corresponding to two fault sizes. The fault sizes for the first bin are -1.0 and -0.8, the fault sizes for the second bin are -0.8 and

-0.6, and so forth; again, these pattern sizes are known from offline simulation.

Once the data or pattern of an unknown anomaly is determined, we can use the interpolation method to determine its corresponding type and size. For a given pair of values of an unknown fault, the normal value is the same, $T_{J0} = 130.1909\,°C$, $T_{T0} = 33.6885\,°C$, $V_{T0} = 126.0445\,m^3$, only the minimum or the maximum value is used to interpolate into each bin to get its corresponding fault size.

Matlab has a command *interp1* which is used for interpolation. For our case, we use $XI = interp1(Y, X, YI, 'linear')$, to find XI: the value of the underlying fault size X at the points in the vector YI. The vector Y specifies the points at which the value X is given, and 'linear' indicates that the method is linear interpolation. In our case, X indicates the known 10 fault sizes which are from -1.0 to $+1.0$ and Y indicates the known datum corresponding to the known fault sizes X. YI indicates the known datum corresponding to the unknown fault size XI, we can use the interpolation method to get the unknown fault size XI. For example, if YI is 42 in Figure 7.2 then *interp1* returns the value $XI = -0.88$.

There are seven faults, and each fault has three outputs, so all faults together have 21 figures. The number of faults are denoted by j, $j = 1 : 7$, and the number of output variables are denoted by i, $i = 1 : 3$. The output variables are heating fluid temperature, measured mix temperature, and measured volume temperature. The known data (pattern sizes) are expressed as Y_{ij}, so Y_{ij} indicates the pattern size of the ith output variable for the jth fault. The Y_{ij}

datum is interpolated into all the figures and corresponding values of X_{ij} are obtained. If for some fault j, $X_{1j} = X_{2j} = X_{3j}$, then we declare that anomaly and fault size are the diagnosis result. If they are different, this fault j is not the underlying anomaly. To account for data and computer accuracy, the match cannot be exact, so we set two thresholds, $\theta_1 = 0.98$ and $\theta_2 = 1.02$. If the ratio of pattern sizes for any two output variables is between θ_1 and θ_2, we can regard them as a match. This is the fault type and size we are seeking.

7.2.3 Interpolation Results

To illustrate this process for an unknown anomaly, the following patterns for the three output variables were provided as a "blind test":

- heating fluid temperature:$[130.1909 \;\; 147.2763]\,°C$
- measured mix temperature:$[33.6885 \;\; 34.9419]\,°C$
- measured volume:$[126.0231 \;\; 126.0445]\,m^3$

The following is the diagnosis result:

The following fault is isolated, as the three output variables have the same size:

The number of the fault = 3

The size of TJ = 0.14981

The size of TT = 0.15

The size of VV = 0.15

In this result, '*The number of the fault = 3*' indicates $j = 3$, '*The size of TJ = 0.14981*' indicates $X_{13} = 0.14981$, '*the size of TT = 0.15*' indicates $X_{23} = 0.15$, and '*the size of VV = 0.15* ' indicates $X_{33} = 0.15$. The ratio of pattern sizes for any two output variables is $\frac{X_{13}}{X_{23}} = 0.9987$, $\frac{X_{13}}{X_{33}} = 0.9987$, and $\frac{X_{23}}{X_{33}} = 1.0$. All the ratios are between θ_1 and θ_2; we can regard them as a match, so the third fault, in which the fault size = 0.15 is what we seek.

7.3 Neuro-Fuzzy Model Practical Application

7.3.1 Objective

The Neuro-Fuzzy model NF_0 provided a good steady-state input/output map, as shown in section 5.3, which enables it to adapt to different conditions. Using the Neuro-Fuzzy models for a real world plant by using only the fault-free model to identify all the faults can eliminate the difficulty of having to train a bank of NF models for all fault scenarios using plant data. Training many NF models from plant data is impractical, the approach described here is feasible.

7.3.2 Producing Pattern Data Using the JCSTR Model

In Figure 7.3, the faulty data $u(t)$ produced by the JCSTR system simulation model are applied to the Neuro-Fuzzy fault-free model, which is denoted by 'NF_0 Model'. The anomaly *F4: Faulty Temperature Sensor Fault* is given as an example to show the method and results. In Figures 7.4, the *circle* variables indicate the output symptoms produced using the Neuro-Fuzzy faulty model, the *star* variables indicate the output symptoms produced using the Neuro-Fuzzy fault-free model, and the *plus* variable

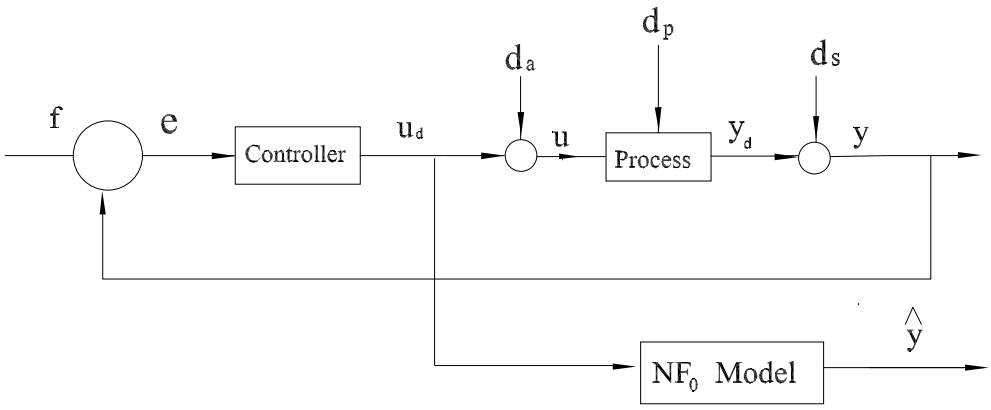

Figure 7.3: Pattern Data Produced by the JCSTR Model

indicates NF model in normal condition.

In Table 7.2, NF_4 indicates the NF faulty temperature sensor model, and NF_0 indicates the NF fault-free model. The results show that they have very similar pattern sizes. Thus, using the Neuro-Fuzzy fault-free model, we can still develop the pattern sizes which we need to identify the anomalies. This approach is also tested successfully on the actuator, which is attached in Appendix D.

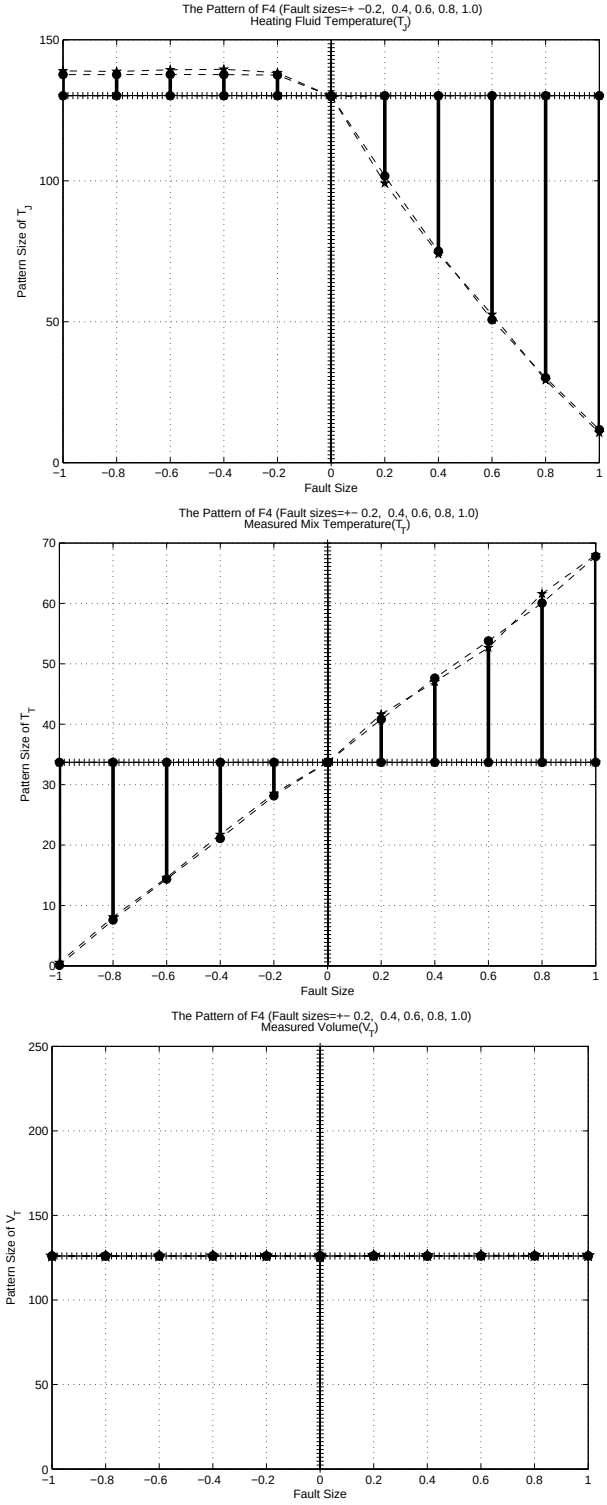

Figure 7.4: Output Variable Patterns for $F4$

Fault Isolation Stage for Fault-free Model NF_0 and Faulty Model NF_4						
	Heating Fluid Temperature $P(T_J) = [\,T_{J0} \quad T_{Jmax}\,]$ or $P(T_J) = [\,T_{Jmin} \quad T_{J0}\,]$, $^\circ C$		Measured Mix Temperature $P(T_T) = [\,T_{T0} \quad T_{Tmax}\,]$ or $P(T_T) = [\,T_{Tmin} \quad T_{T0}\,]$, $^\circ C$		Measured Volume $P(V_T) = [\,V_{T0} \quad V_{Tmax}\,]$ or $P(V_T) = [\,V_{Tmin} \quad V_{T0}\,]$, m^3	
NF Model	Fault Size	Pattern Size	Fault Size	Pattern Size	Fault Size	Pattern Size
NF_4	-0.2	[130.1909 137.4885]	-0.2	[28.1407 33.6885]	-0.2	[126.0445 126.0913]
NF_4	-0.4	[130.1909 137.6755]	-0.4	[21.0861 33.6885]	-0.4	[125.9895 126.0445]
NF_4	-0.6	[130.1909 137.6915]	-0.6	[14.3610 33.6885]	-0.6	[125.9163 126.0445]
NF_4	-0.8	[130.1909 137.6677]	-0.8	[7.5943 33.6885]	-0.8	[126.0445 126.0867]
NF_4	-1.0	[130.1909 137.6796]	-1.0	[0.0855 33.6885]	-1.0	[126.0445 126.0899]
NF_4	0.2	[101.6876 130.1909]	0.2	[33.6885 40.8116]	0.2	[126.0107 126.0445]
NF_4	0.4	[75.0056 130.1909]	0.4	[33.6885 47.6371]	0.4	[126.0253 126.0445]
NF_4	0.6	[50.6876 130.19091]	0.6	[33.6885 53.7948]	0.6	[126.0174 126.0445]
NF_4	0.8	[30.1266 130.1909]	0.8	[33.6885 60.0501]	0.8	[125.9824 126.0445]
NF_4	1.0	[11.6876 130.1909]	1.0	[33.6885 67.7864]	1.0	[125.8639 126.0445]
NF_0	-0.2	[130.1909 138.3555]	-0.2	[28.5322 33.6885]	-0.2	[126.0445 126.1258]
NF_0	-0.4	[130.1909 139.5521]	-0.4	[21.7367 33.6885]	-0.4	[126.0445 126.1185]
NF_0	-0.6	[130.1909 139.3562]	-0.6	[14.6028 33.6885]	-0.6	[125.8754 126.0445]
NF_0	-0.8	[130.1909 138.7673]	-0.8	[8.0678 33.6885]	-0.8	[126.0445 126.1139]
NF_0	-1.0	[130.1909 138.9756]	-1.0	[0.5365 33.6885]	-1.0	[126.0445 126.1021]
NF_0	0.2	[99.1389 130.1909]	0.2	[33.6885 41.6589]	0.2	[126.0445 126.1203]
NF_0	0.4	[74.0199 130.1909]	0.4	[33.6885 47.0218]	0.4	[126.0445 126.0534]
NF_0	0.6	[52.5622 130.1909]	0.6	[33.6885 52.6854]	0.6	[126.0445 126.0452]
NF_0	0.8	[29.2541 130.1909]	0.8	[33.6885 61.5897]	0.8	[125.9842 126.0445]
NF_0	1.0	[10.5892 130.1909]	1.0	[33.6885 68.0182]	1.0	[125.9412 126.0445]

Table 7.2: Fault Isolation Stage for NF_0 and NF_4

7.3.3 Producing Pattern Data Using Sensor and Actuator Matrices

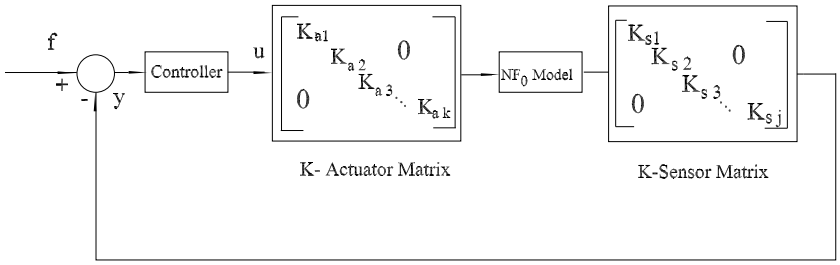

Figure 7.5: Pattern Data Produced by Actuator and Sensor Matrices System

In Figure 7.5, the faulty patterns are produced by appropriately setting the actuator matrix or sensor matrix for each fault in the real plant. The K-Actuator Matrix is used to model all the actuator faults: the diagonal elements are $K_{a1}, ...K_{ak}$, where k indicates the number of each actuator. If any K_{ai} ($i \in 1, \ldots, k$) is not unity, the kth actuator is faulty, e.g, $K_{a2} = 0.8$ corresponding to a -20 percent fault in actuator 2. In our case, the K-Actuator Matrix corresponds to the five inputs. The K-Sensor Matrix is used to model all the sensor faults in a similar way. The diagonal elements are $K_{s1}, ...K_{sj}$, where j indicates the number of each sensor. In our case, $j = 1, 2, 3$ corresponding to the three output variables. The faulty pattern sizes are produced by the K-Actuator Matrix and K-Sensor Matrix in series with the Neuro-Fuzzy fault-free model and controller in a closed-loop configuration (Figure 7.5). The results should show that it produces similar results with the former method, so we should not require numerous NF faulty models, we can just use the fault-free NF model. This study remains to be done as future work.

Chapter 8

Thesis Observations

8.1 Summary and Conclusions

1. The literature review of FDI using quantitative model-based approaches, qualitative model-based approaches, and process history-based approaches has been outlined in this thesis.

2. The concept and construction of Neuro-Fuzzy systems have been systematically explained.

3. For a JCSTR system, Neuro-Fuzzy models have been implemented to diagnose single faults, and their robustness to setpoint change was tested. It is a new approach that not only can diagnose the sensor and actuator faults, but also can diagnose disturbances.

4. Neuro-Fuzzy models were also tested to diagnose sequential faults, which is a novel approach.

5. The Neuro-Fuzzy model approach was extended to identify faults of arbitrary size, extending robustness by developing nonlinear symptom mapping interpolations, which is also a novel technique.

6. Finally, as another novel approach, deriving the Neuro-Fuzzy models NF_k for the real world plant by using only the fault-free model to identify all the fault symptoms eliminated the problem of having to train a large bank of NF models for all fault scenarios.

8.2 Future Work

The future work is to use the Neuro-Fuzzy fault-free model to identify the faults using the faulty data produced by the K-Actuator Matrix and K-Sensor Matrix, as outlined in section 7.3.3. It should produce similar results with the former method, so we need not use many NF faulty models, just use the NF fault-free model.

Bibliography

[1] Aleksander, I. and H. Morton. (1990). *An Introduction to Neural Computing.* Chapman and Hall. New York.

[2] Ayoubi, R. (1995). Neuro-fuzzy structure for rule generation and application in the fault diagnosis of technical processes. *Proc. American Control Conference* Washington, DC, pp. 1757-2761.

[3] Balle, P., D. Fussel, and O. Hecker. (1997). Detection and isolation of sensor faults for nonlinear processes based on local linear models. *Proc. American Control Conference*, Albuquerque, NM, pp. 468-472.

[4] Brown, M. and C. Harris. (1994). *Neurofuzzy adaptive modeling and control.* Prentice Hall. New York.

[5] Frank, P. M. (1990). Fault diagnosis in dynamic systems using analytical and knowledge-based redundancy: A Survey and some new results. *Automatica. Vol. 26.* No. 3. pp. 459-474.

[6] Fussel, D., P. Balle, and R. Isermann. (1997). Closed loop fault diagnosis based on a nonlinear process model and automatic fuzzy rule generation. *Prep. IFAC Symp. SAFEPROCESS*, Kingston upon Hull. U.K.

[7] Gertler, J. (1998). *Fault detection and diagnosis in engineering systems.* Marcel Dekker. Fairfax, Virginia.

[8] Leonard, J. A. and M. A. Kramer. (1993). Diagnosing dynamic faults using modular neural nets. *IEEE Expert Syst. Mag. Vol. 8.* No. 2, pp. 44-53.

[9] Lunze, J. and J. Schroder. (1999). Application of qualitative observation and prediction to a neutralization process. *Proc. 14th IFAC World Congress, Vol. I.* Beijing, China, pp. 49-54.

[10] Naidu, S., E. Zarou, and T. J. McAvoy. (1990). Use of neural-networks for failure detection in a control system. *IEEE Contr. Syst. Magazine. Vol. 10.* pp. 49-55.

[11] Patton, R. J. (1999). *Robust Model-Based Fault Diagnosis for Dynamic Systems.* Kluwer Academic Publishers. Hull. U.K.

[12] Sayda, Atalla F. (2005). A Benchmark Model of a Jacketed Stirred Tank Heater for Fault Detection and Isolation. *Private Communication.* University of New Brunswick, Fredericton, NB, Canada.

[13] Shen, Q. and R. Leitch. (1993). Fuzzy Qualitative Simulations. *IEEE Trans. on Syst. Man and Cybern. Vol. SMC-23.* No. 4, pp. 1038-1061.

[14] Sugeno, M. and G. T. Kang. (1988). Structure identification of fuzzy model. *Fuzzy sets and systems. Vol. 28.* pp. 15-33.

[15] Takagi, T. and M. Sugeno. (1985). Fuzzy identification of system and its applications to modeling and control. *IEEE Trans. on System Man and Cybern. Vol. SMC-15* pp. 116-132.

[16] Wang, L.-X. (1992). Fuzzy systems are universal approximators. *Proc. IEEE Int. Conf. Fuzzy System.* San Diego, CA.

Appendix A

A Benchmark Model of a Stirred Tank Heater

A.1 Objective

Consider a jacketed stirred tank heater reactor as shown in Figure A.1, where the tank inlet stream is received from another process unit. The objective is to raise the temperature of the inlet stream to a desired value and maintain volume in the tank at a specific setpoint. A heat transfer fluid is circulated through a jacket to heat the fluid in the tank. In some processes steam is used as the heat transfer fluid and most of the energy transported is due to the phase change of steam to water. In other processes a heat transfer fluid is used where there is no phase change. In this module we assume that no change of phase occurs in either the tank fluid or the jacket fluid. We also do not consider chemical reactions in this model.

A.2 Developing the Dynamic Model

1 In order to find the dynamic modeling equations of the tank and jacket temperatures, we make the following assumptions:

- Constant volume and liquids with constant density and heat capacity.
- Perfect mixing in both the tank and jacket.

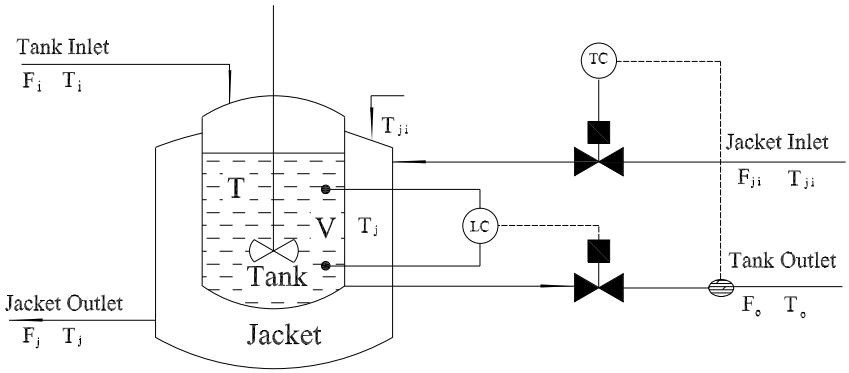

Figure A.1: Jacketed Continuously Stirred Tank Reactor (JCSTR)

- The tank inlet flow rate, jacket flow rate, tank inlet temperature and jacket inlet temperature may change (these are the inputs).
- The rate of heat transfer from the jacket to the tank is governed by the equation, $Q = UA(T_j - T)$, where U is the overall heat transfer coefficient and A is the area for heat transfer.

2 The following are the variables :

- A: Area for heat transfers
- C_p: heat capacity (energy/mass*temp)
- F: Volumetric Flow rate (volume/ time)
- ρ: Density (mass/volume)
- T: Temperature
- t: time
- Q: rate of heat transfer (energy/time)
- τ: heat transfer coefficient (energy/time*area*temp)
- V: volume

3 The following are the subscripts:

- i: inlet
- j: jacket
- ji: jacket inlet
- ref: reference state
- s: steady-state

4 Equations:

- Material balance around tank: accumulation = inflow - outflow;

$$\frac{dV\rho}{dt} = F_i\rho - F\rho \tag{A.1}$$

- Thermal energy balance around tank: accumulation = heat in inflow + heat via heat transfer - heat in outflow.

$$\frac{dV\rho C_\rho(T - T_{ref})}{dt} = F\rho_i C_\rho(T_i - T_{ref}) + Q - F\rho C_\rho(T - T_{ref})$$

$$Q = UA(T_i - T)$$

$$\frac{dT}{dt} = \frac{F}{V}(T_i - T) + \frac{UA(T_J - T)}{V\rho C_\rho} \tag{A.2}$$

- Energy balance in the jacket: accumulation =heat in inflow + heat via heat transfer - heat in outflow:

$$\frac{d(V_j\rho_j C_{\rho j}(T_j - T_{ref}))}{dt} = F_j\rho_j C_{\rho j}(T_{ji} - Tref) - Q - F_j\rho_j C_{\rho j}(T_j - T_{ref})$$

$$Q = UA(T_i - T)$$

$$\frac{dT_j}{dt} = \frac{F_j}{V_j}(T_{ji} - T_j) + \frac{UA(T_j - T)}{V_j\rho_j C_{\rho j}} \tag{A.3}$$

Equations A.1 to Equation A.3 represent the open loop nonlinear model of the JCSTR heater.

5 The design parameters are the following:

Diameter of the reactor (m): $D_r = 5$

Reactor Height (m): $H_r = 2D_r$

Reactor volume (m^3):

$$V_r = \frac{pi}{2}(D_r^3)$$

Area for heat transfer (m^2):

$$A = \frac{9}{4}pi(D_r^2)$$

Heat capacity (j/kgK): $C_\rho = 4.1868 * 1000$

Mixture inflow (m^3/s): $F_{in} = 0.1$

Mixture Outflow (m^3/s): $F_{out} = 0.1$

Mixture Volume (m^3): $V = 180$

Density (kg/m^3): $\rho = 997.95$

Temperature of the mixture feed (K): $T_{in} = 10 + 273$

Temperature of the mixture (K): $T_{ss} = 34.7602 + 273$

Heating water inflow (m^3/s) : $F_{jin} = 0.15$

Heating water Outflow (m^3/s): $F_{jout} = 0.15$

Heating water Volume (m^3): $V_j = 9$

Temperature of the heating water feed (K): $T_{jin} = 120 + 273$

Temperature of the heating water (K): $T_j = 103.4932 + 273$

Heat Transfer coefficient $(W/m^2.K)$: $U = 851.74$

Temp proportional gain: $K_{pt} = 0.033114$

Temp integral gain: $K_{it} = 4.5929e - 005$

Volume proportional gain: $K_{pv} = 0.0024$

Volume integral gain: $K_{iv} = 1.4621e - 006$

Appendix B

Complementary Results of Single Fault Diagnosis in JCSTR System

B.1 The Detection Stage of the Neuro-Fuzzy Model in the Nominal Case

In this case, the normal operating point of the volume and temperature are nominal ($dV_{sp} = 0$, $dT_{sp} = 0$). We use the NF models to diagnose the single anomaly. In Figure B.1 to Figure B.4, The *plus* variables indicate the NF model output under normal conditions, and the *star* variables indicate the system process output in abnormal conditions. From the results, all the anomalies can be detected if they occur one at a time.

Figure B.1 (a) shows the effect of a high mix inflow disturbance which increases by 50 percent at hour 2. The heating fluid temperature increases to 5 percent, the measured mix temperature decreases to 15 percent, and the measured volume increases to 8 percent. Thus all of the three output variables have changes.

Figure B.1 (b) shows the effect of a low inlet temperature disturbance which decreases by 50 percent at hour 2. The heating fluid temperature increases to 5 percent, the measured mix temperature decreases to 8 percent, and the measured volume has no change.

Again, Figure B.2 and Figure B.4 show that the detection is successful for each anomaly.

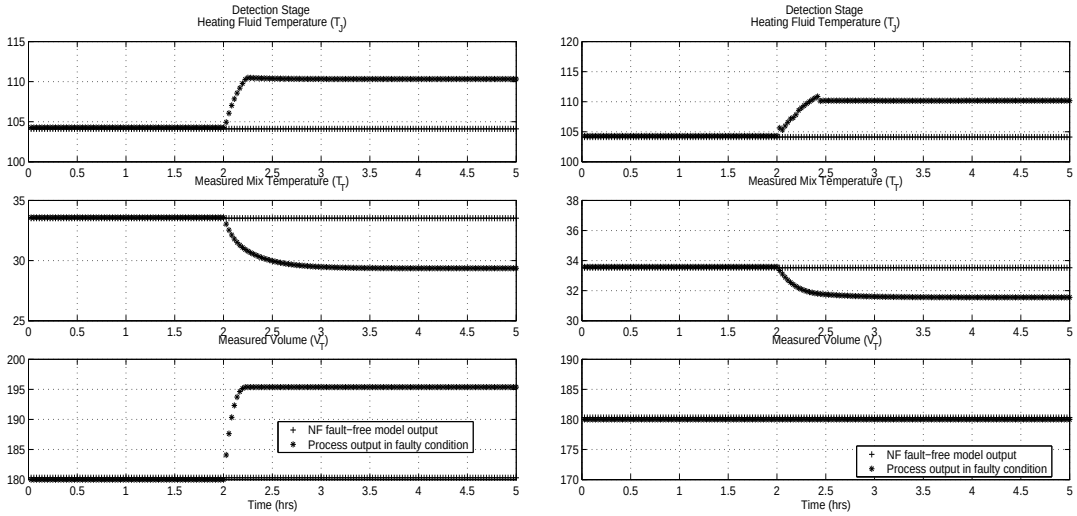

(a) Anomaly 2 (b) Anomaly 3

Figure B.1: Anomaly Detection in Nominal Case

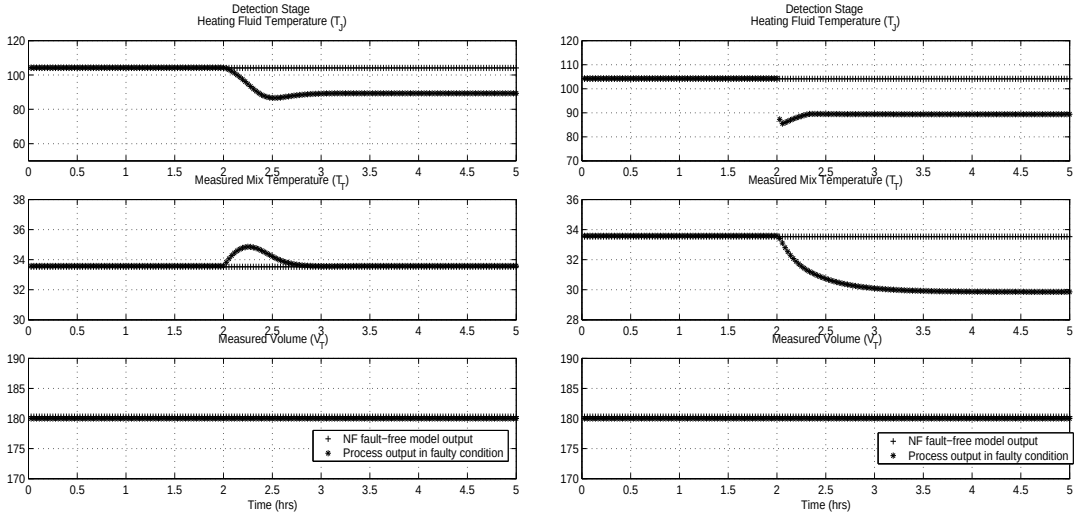

(a) Anomaly 4 (b) Anomaly 5

Figure B.2: Anomaly Detection in Nominal Case

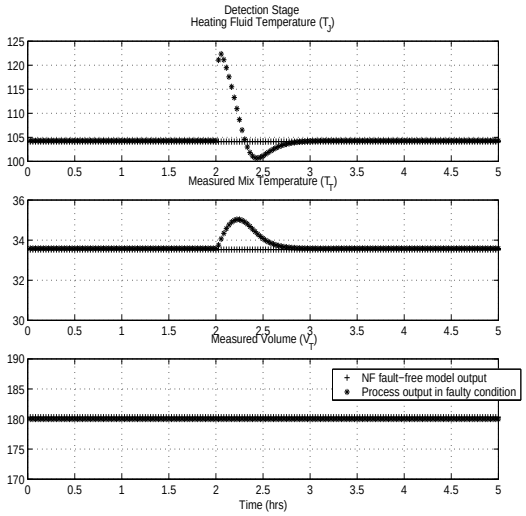

(a) Anomaly 6

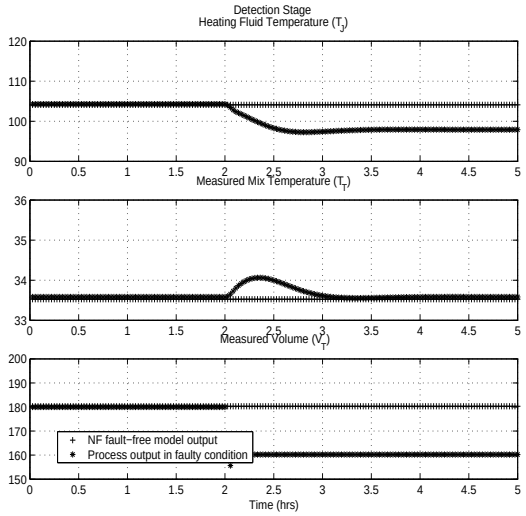

(b) Anomaly 8

Figure B.3: Anomaly Detection in Nominal Case

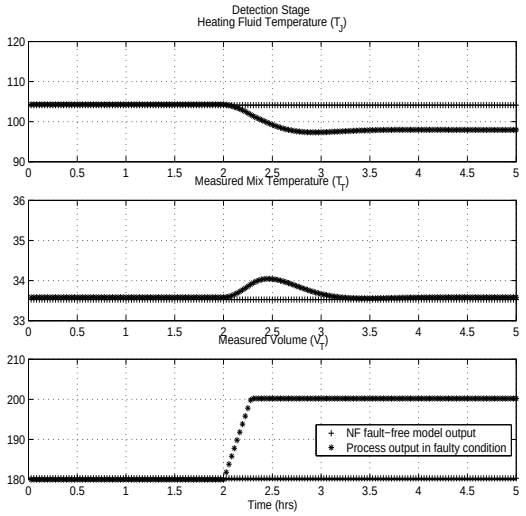

(a) Anomaly 9

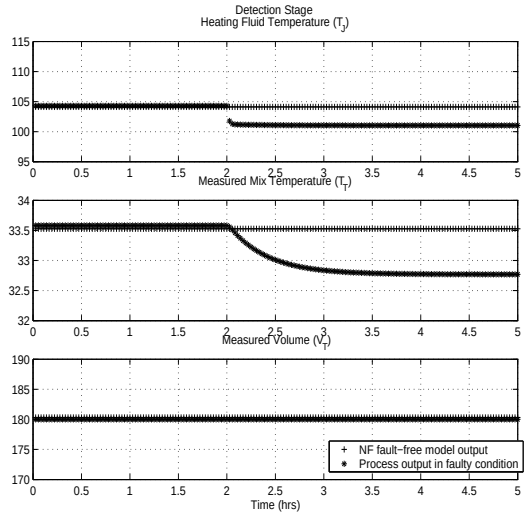

(b) Anomaly 10

Figure B.4: Anomaly Detection in Nominal Case

B.2 The Detection Stage of Ten Percent Offset Case

In this section, the operating point of the measured volume is decreased 10 percent ($dV_{sp} = -18\,m^3$), the measured mix temperature is also decreased 10 percent ($dT_{sp} = -3.35\,°C$), and we use the same Neuro-Fuzzy models to diagnose anomalies under this level of offset. Figure B.5 to Figure B.8 illustrate that detection is successful for each anomaly.

Figure B.5 (a) shows the effect of a high mix inflow disturbance which increases by 50 percent at hour 2. The heating fluid temperature increases to 14 percent, the measured mix temperature decreases to 6 percent, and the measured volume increases to 10 percent. Thus all of the three output variables have changes.
Figure B.5 (b) shows the effect of a low inlet temperature disturbance which decreases by 50 percent at hour 2. The heating fluid temperature increases to 14 percent, the measured mix temperature decreases to 4 percent, and returns to normal condition gradually, and the measured volume has no change.

Once more, Figure B.6 to Figure B.8 show that the detection is successful for each anomaly.

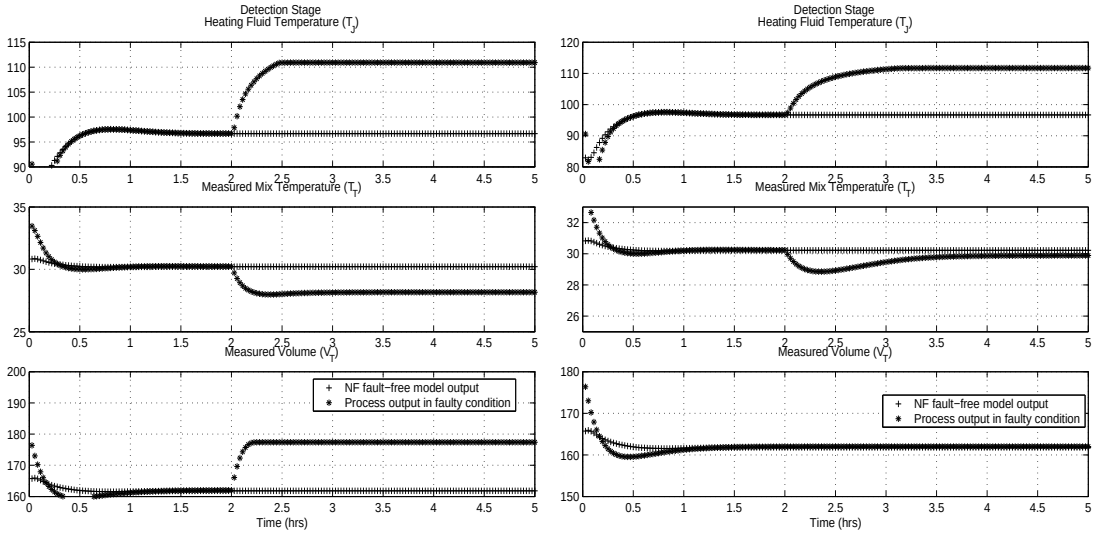

(a) Anomaly 2 (b) Anomaly 3

Figure B.5: Anomaly Detection at Ten Percent Offset

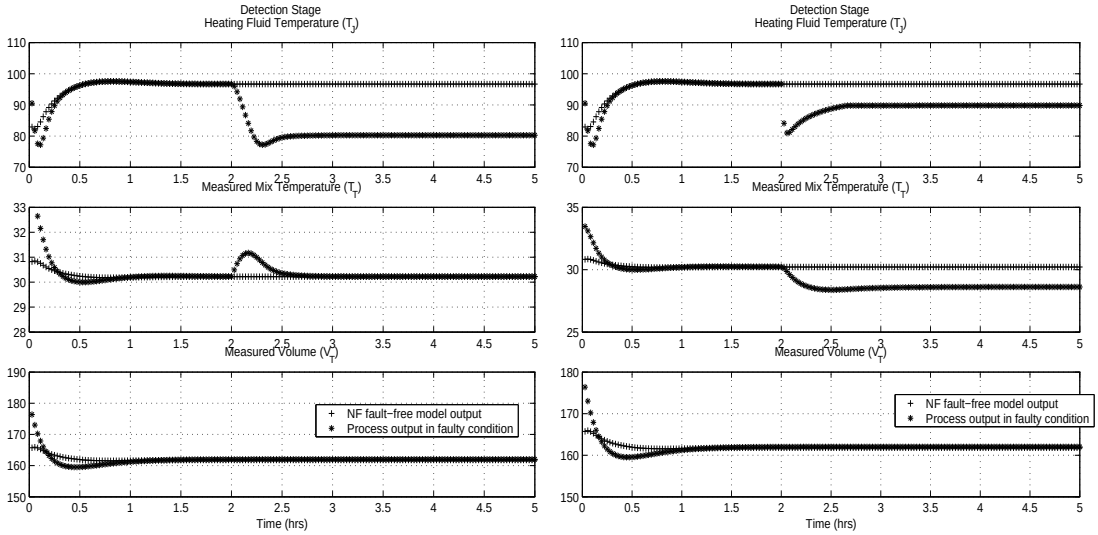

(a) Anomaly 4 (b) Anomaly 5

Figure B.6: Anomaly Detection at Ten Percent Offset

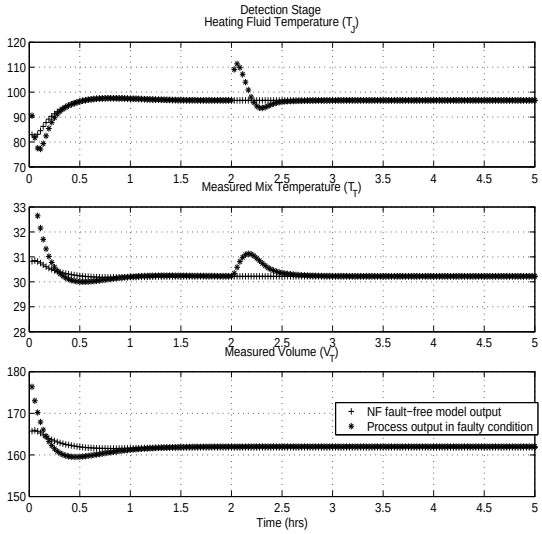

(a) Anomaly 6

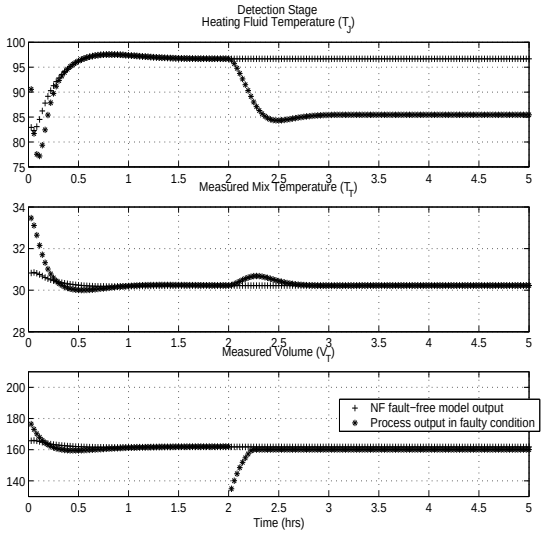

(b) Anomaly 8

Figure B.7: Anomaly Detection at Ten Percent Offset

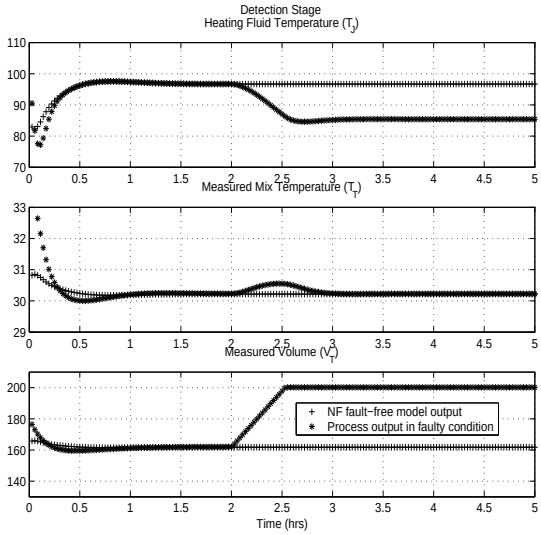

(a) Anomaly 9

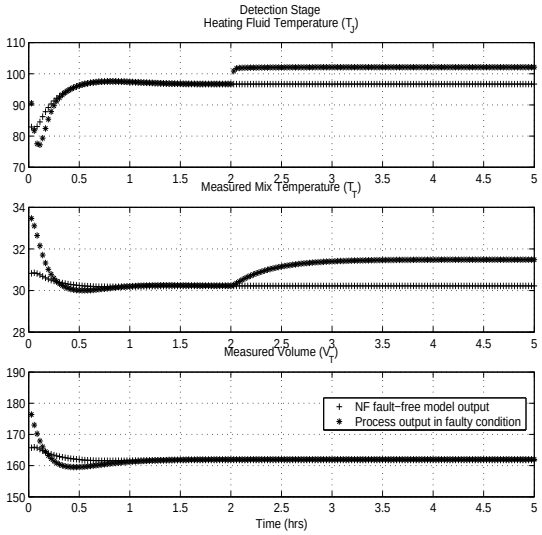

(b) Anomaly 10

Figure B.8: Anomaly Detection at Ten Percent Offset

B.3 The Detection Stage of Thirty Percent Offset Case

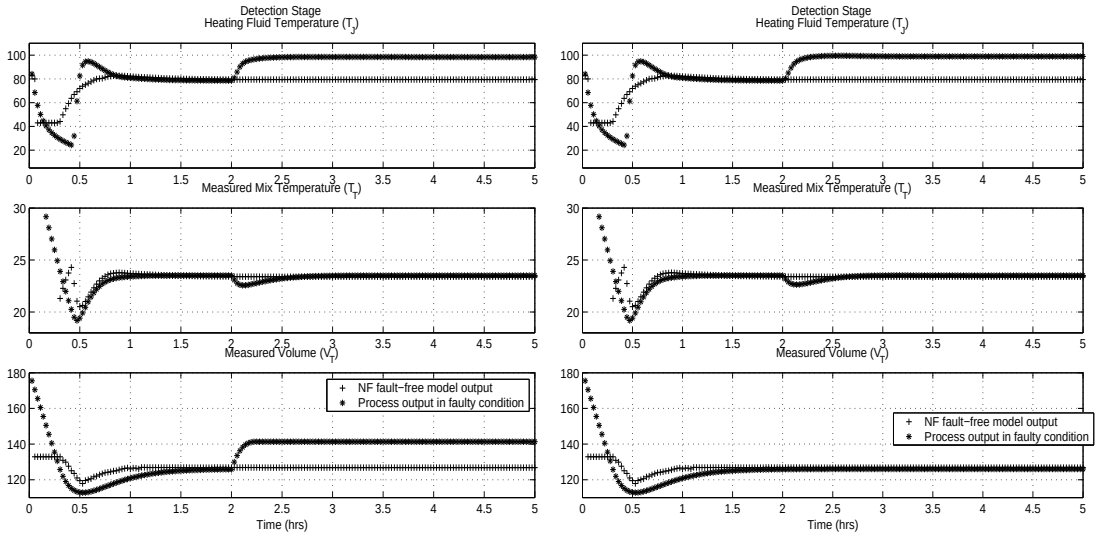

(a) Anomaly 2 (b) Anomaly 3

Figure B.9: Anomaly Detection in Thirty Robustness Case

In this study, when the operating point of the measured volume is decreased 30 percent ($dV_{sp} = -54\,m^3$), and the measured mix temperature is also decreased 30 percent ($dT_{sp} = -10\,^\circ C$), and we use the same Neuro-Fuzzy models to diagnose anomalies under this level of offset. Figure B.9 to Figure B.11 illustrate the detection stage. As before, detection is successful for each anomaly.

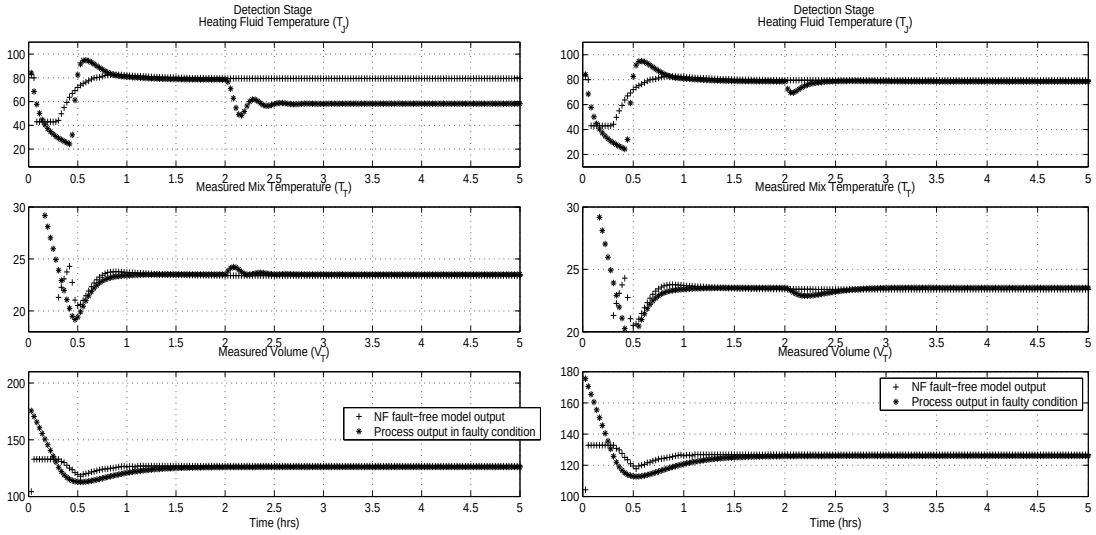

(a) Anomaly 4 (b) Anomaly 5

Figure B.10: Anomaly Detection in Thirty Robustness Case

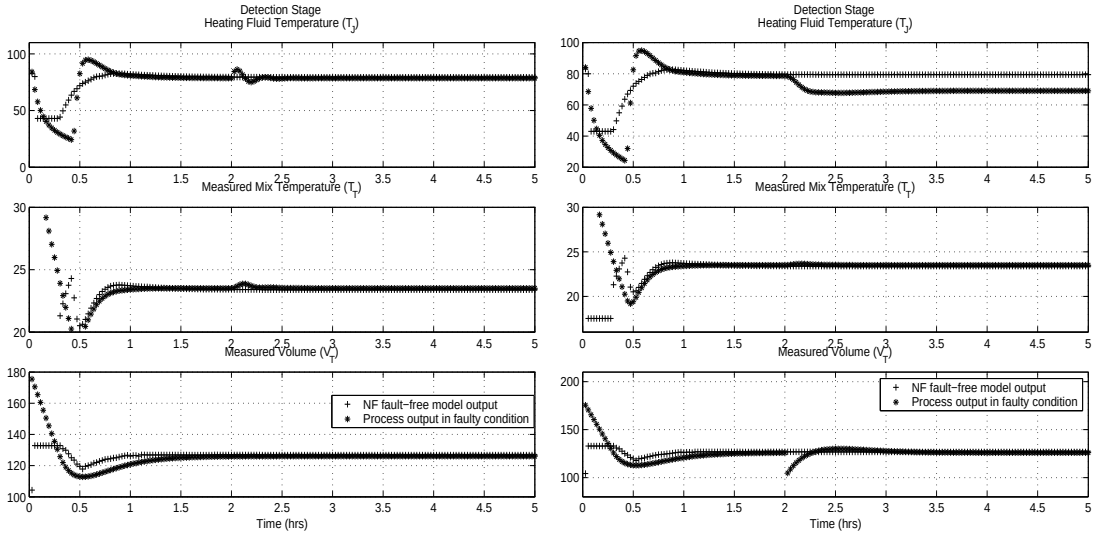

(a) Anomaly 6 (b) Anomaly 8

Figure B.11: Anomaly Detection in Thirty Robustness Case

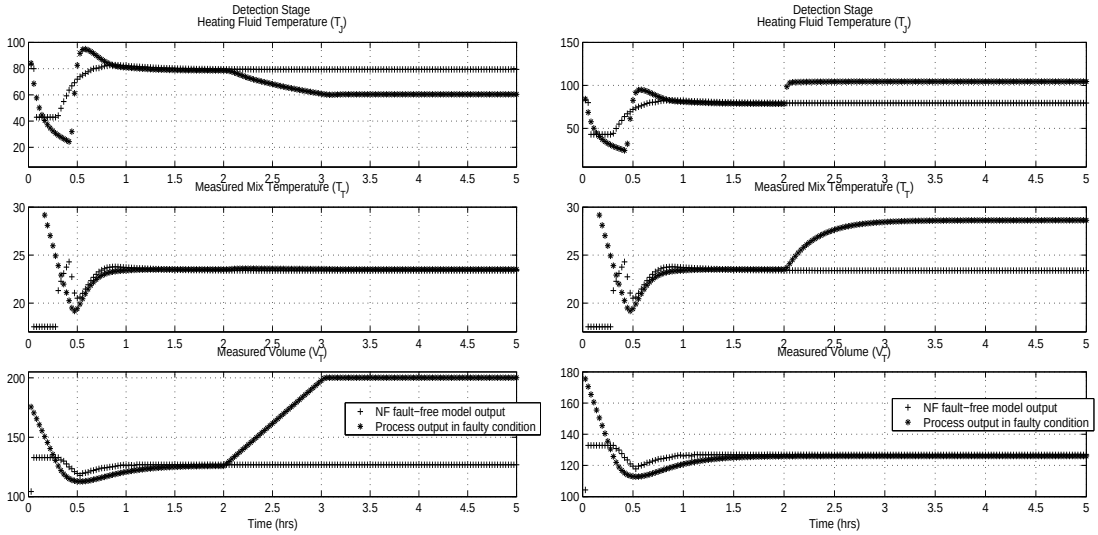

(a) Anomaly 9 (b) Anomaly 10

Figure B.12: Anomaly Detection in Thirty Robustness Case

B.4 The Isolation Stage of Thirty Percent Offset Case

Figure B.13 to Figure B.15 shows the first isolation stage. From hour 2.1, we can isolate 2nd, 3rd, 5th, and 8th anomalies soon after they occur.

Figure B.15 to Figure B.17 illustrates the second isolation stage. From hour 2.5, we can isolate the 4th, 6th, 7th, and 10th anomalies within half hour after they occur.

Figure B.17 illustrates the third isolation stage. From hour 3, we can isolate the 1st and 9th anomalies within one hour after they occur.

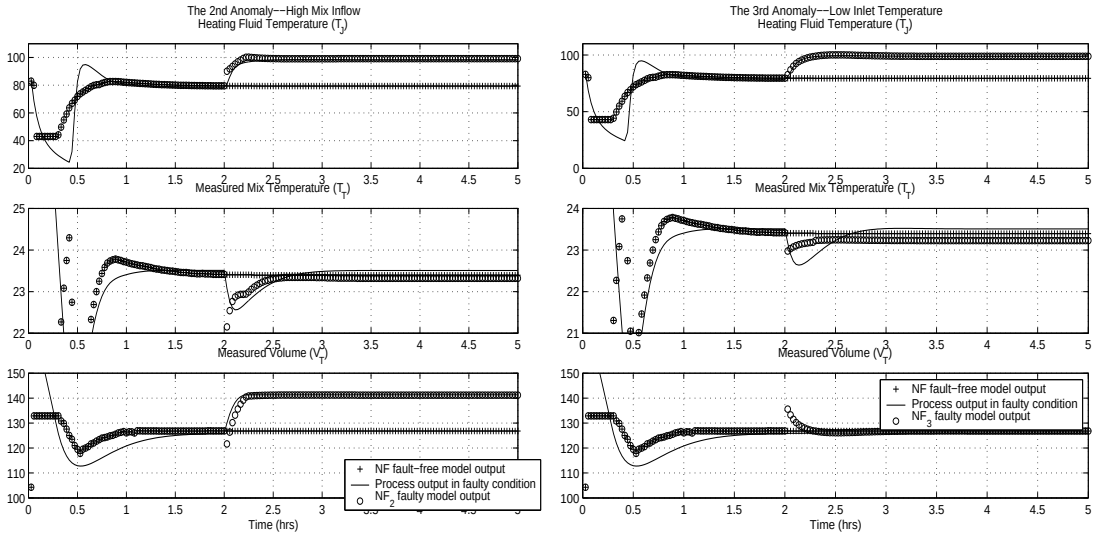

(a) Anomaly 2 (b) Anomaly 4

Figure B.13: Anomaly Isolation Stage 1 at Thirty Percent Offset

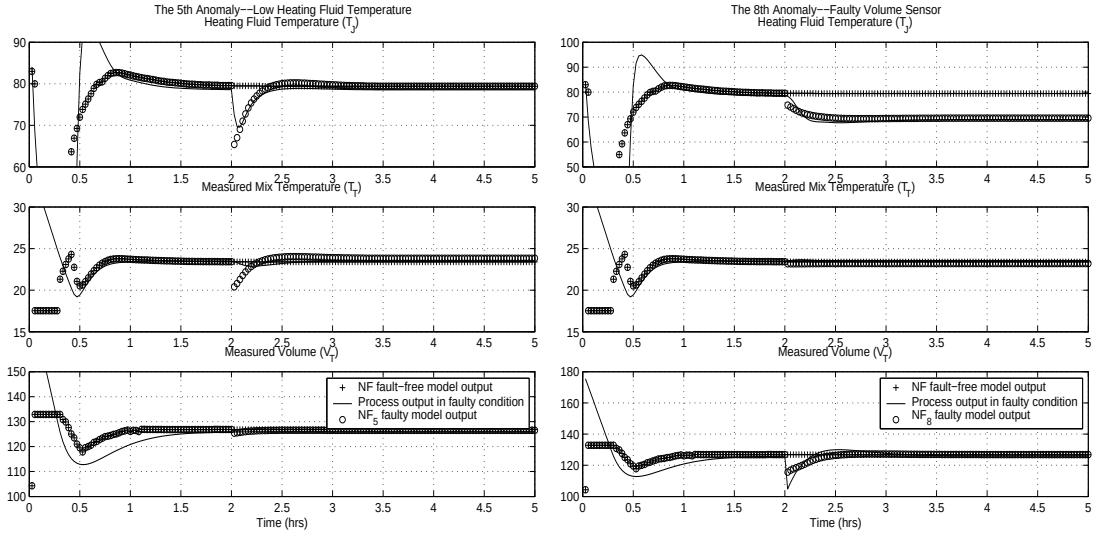

(a) Anomaly 5 (b) Anomaly 8

Figure B.14: Anomaly Isolation Stage 1 at Thirty Percent Offset

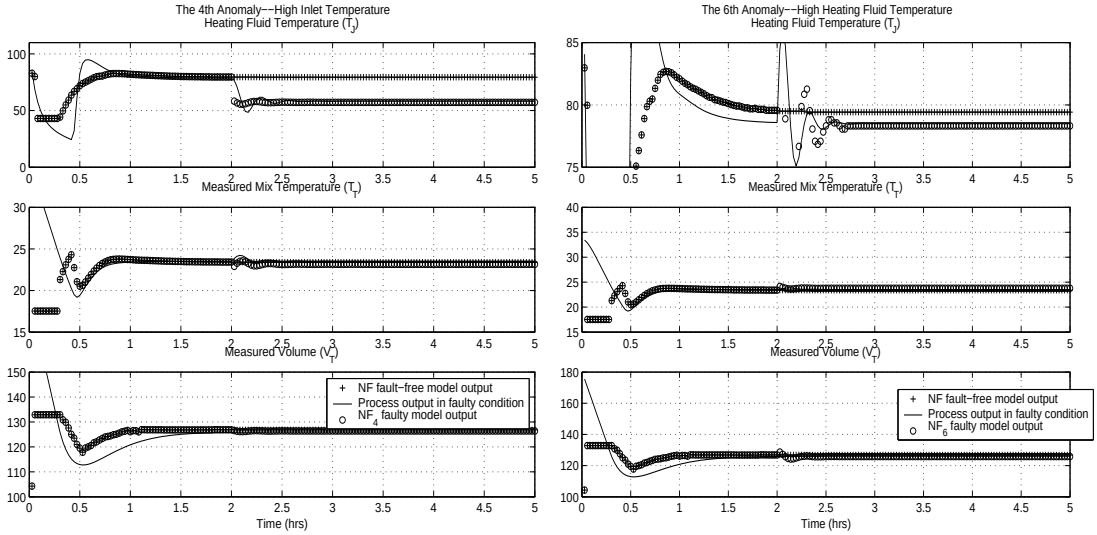

(a) Anomaly 4 (b) Anomaly 6

Figure B.15: Anomaly Isolation Stage 2 at Thirty Percent Offset

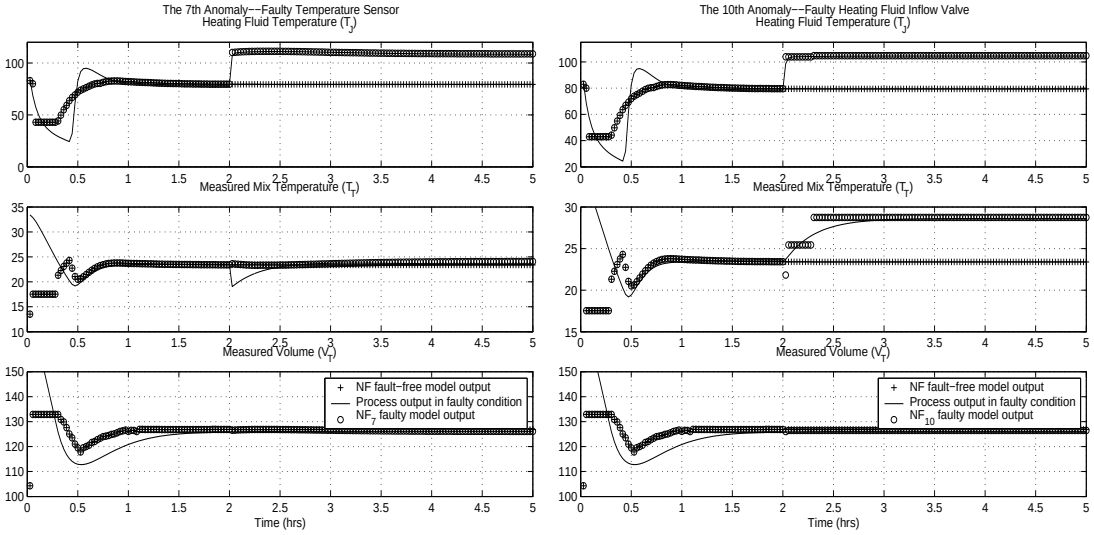

(a) Anomaly 7 (b) Anomaly 10

Figure B.16: Anomaly Isolation Stage 2 at Thirty Percent Offset

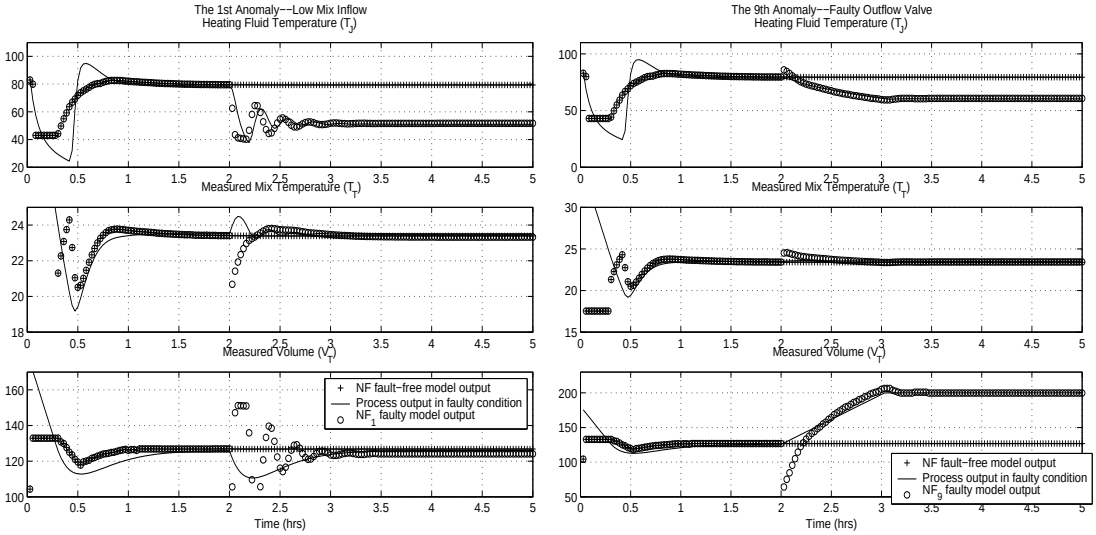

(a) Anomaly 1 (b) Anomaly 9

Figure B.17: Anomaly Isolation Stage 3 at Thirty Percent Offset

Appendix C

Complementary Results of Sequential Faults diagnosis in JCSTR System

C.1 Detection of the Sequential Faults

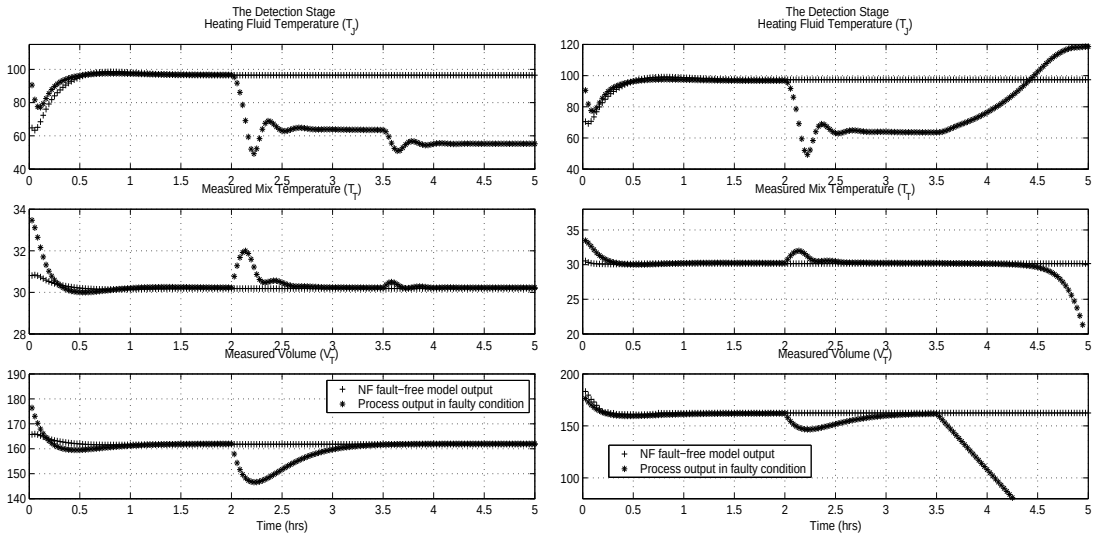

(a) Anomalies F_1 Then F_4 (b) Anomalies F_1 Then F_9

Figure C.1: The Detection Stage Case

The following simulation results illustrate that we use the NF models to detect the sequential faults.

In Figure C.1, the *plus* variables indicate the Neuro-Fuzzy Model in normal conditions and the *star* variables indicate the process in faulty conditions. In the following two examples, at hour 2, the first anomaly occurs, and at hour 3.5, the second anomaly occurs in sequence.

Figure C.1 (a) shows that two anomalies occur sequentially. The first anomaly is the low mix inflow disturbance which occurs at hour 2. The second anomaly is the high inlet temperature disturbance, which occurs at hour 3.5.

1. After hour 2, the first output, heating fluid temperature decreases below the normal condition. After hour 3.5, the first output decreases again, due to the second anomaly.

2. After hour 2, the second output, measured mix temperature increases a little above the normal condition and quickly returns to normal condition. After hour 3.5, there is a small transient; it seems the second anomaly has very little effect on the state of the measured mix temperature variable.

3. After hour 2, the third output, measured volume decreases below the normal condition and then gradually returns to normal condition. After hour 3.5, the third output stays normal. It is not affected by the second anomaly.

Figure C.1 (b) shows that two anomalies occur sequentially. The first anomaly is the low mix inflow disturbance, which occurs at hour 2. The second anomaly is the faulty outflow valve, which occurs at hour 3.5.

1. At hour 2, the first output, heating fluid temperature, decreases below the normal condition. At hour 3.5, the first output suddenly increases greatly and rises above the normal condition, due to the second anomaly.

2. At hour 2, the second output, measured mix temperature increases a little,

decreases again, and quickly returns to normal condition. At hour 3.5, the second output gradually decreases below the normal condition, due to the second anomaly.

3. At hour 2, the third output, measured volume decreases below normal condition and then gradually returns to normal condition. At hour 3.5, the third output decreases to normal condition due to the second anomaly.

In the detection stage, from hour 0 to hour 2, the Neuro-Fuzzy model is in normal condition, so there is no anomaly in the system. Based on the fault-free Neuro-Fuzzy model NF_0, by hour 2, we detected the first anomaly, then by hour 3.5, another anomaly is detected.

C.2 Isolation of the Sequential Faults

In this section, we will see how the Neuro-Fuzzy model can isolate the sequential faults after they occur. In Figure C.2, the *plus* variables indicate the NF model output in normal conditions, the *circle* variables indicate the Neuro-Fuzzy model outputs of sequential faults, and the *solid* variables indicate the system process outputs in faulty conditions. The *solid* variables are used to determine whether NF faulty models have good performance. The first anomaly occurs from hour 2 to hour 3.5, the second anomaly occurs from hour 3.5 to hour 5.

Table C.1 and Table C.2 show the isolation stages of the sequential faults, using the Neuro-Fuzzy models. For the three output variables, as before, each variable is defined by two values, and corresponding patterns are denoted by '0', '-', '–', '+', etc., as before.

For the sequential anomalies in Figure C.2 (a), the first anomaly is isolated at hour 2.5, the heating fluid temperature decreases, the measured mix temperature increases

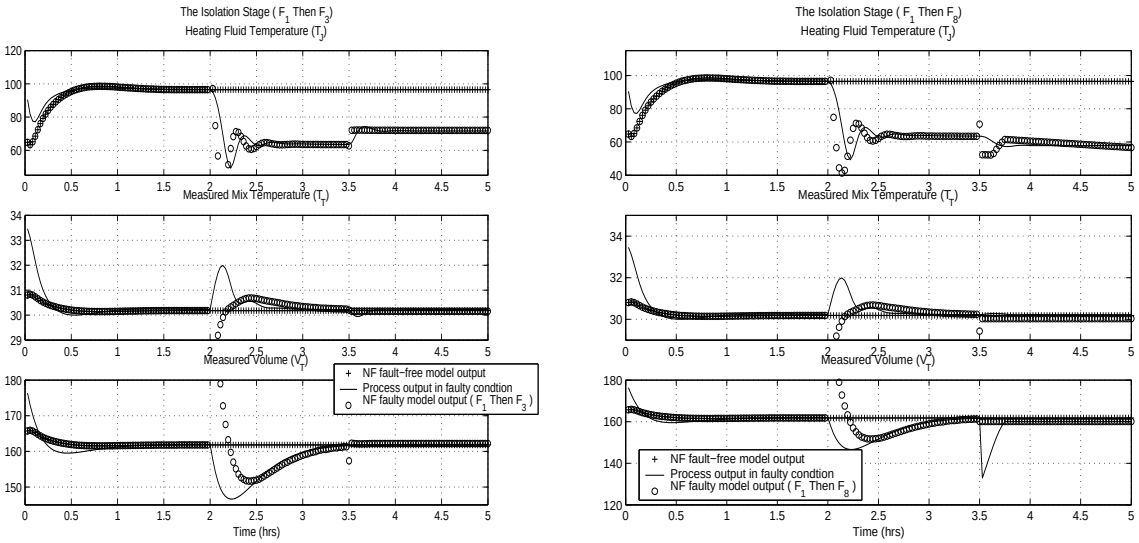

(a) Anomalies F_1 Then F_3 (b) Anomalies F_1 Then F_8

Figure C.2: Sequential Faults Isolation Stage

Sequential Fault Isolation Stage, F_1 Then F_3						
	Heating Fluid Temperature $P(T_J) = [\,T_{J0} \quad T_{Jmax}\,]$ or $P(T_J) = [\,T_{Jmin} \quad T_{J0}\,]$, $^\circ C$		Measured Mix Temperature $P(T_T) = [\,T_{T0} \quad T_{Tmax}\,]$ or $P(T_T) = [\,T_{Tmin} \quad T_{T0}\,]$, $^\circ C$		Measured Volume $P(V_T) = [\,V_{T0} \quad V_{Tmax}\,]$ or $P(V_T) = [\,V_{Tmin} \quad V_{T0}\,]$, m^3	
Anomaly	Pattern	Size	Pattern	Size	Pattern	Size
1st	$--$	[61.0641 96.6733]	0	[30.2185 30.6767]	$-\Rightarrow 0$	[151.8216 161.7959]
3th	$--$	[72.2108 96.6733]	0	[30.1571 30.2185]	0	[161.7959 162.1122]

Table C.1: Sequential Faults Isolation Stage, F_1 Then F_3

Sequential Fault Isolation Stage, F_1 Then F_8						
	Heating Fluid Temperature $P(T_J) = [\,T_{J0} \quad T_{Jmax}\,]$ or $P(T_J) = [\,T_{Jmin} \quad T_{J0}\,]$, $^\circ C$		Measured Mix Temperature $P(T_T) = [\,T_{T0} \quad T_{Tmax}\,]$ or $P(T_T) = [\,T_{Tmin} \quad T_{T0}\,]$, $^\circ C$		Measured Volume $P(V_T) = [\,V_{T0} \quad V_{Tmax}\,]$ or $P(V_T) = [\,V_{Tmin} \quad V_{T0}\,]$, m^3	
Anomaly	Pattern	Size	Pattern	Size	Pattern	Size
1st	$--$	[61.0641 96.6733]	0	[30.2185 30.6767]	$-\Rightarrow 0$	[151.8216 161.7959]
8th	$---$	[53.1220 96.6733]	0	[30.0289 30.2185]	0	[160.0693 161.7959]

Table C.2: Sequential Faults Isolation Stage, F_1 Then F_8

and quickly returns to normal, and the measured volume decreases and then returns to normal condition. Table C.1 shows the pattern and size of the first anomaly. This anomaly is low mix inflow disturbance, the 1st anomaly of the ten anomalies.

At hour 3.6, Figure C.2 (a) shows that the three output variables begin to change due to the second anomaly. The heating fluid temperature increases, the measured mix temperature does not change, and the measured volume does not change. Table C.2 shows the pattern and size of the second anomaly, which matches the pattern of model $NF_{1,3}$, so we isolate the anomaly as low inlet temperature disturbance, the 3th anomaly of the ten anomalies. These two anomalies have different patterns and sizes, so we can isolate this sequential faults after they occur.

For the sequential anomalies in Figure C.2 (b), the first anomaly is isolated at hour 2.5, the heating fluid temperature decreases, the measured mix temperature increases and quickly returns to normal, and the measured volume decreases and then returns to normal condition. Table C.2 shows the pattern and size of the first anomaly. This anomaly is low mix inflow disturbance, the 1st anomaly of the ten anomalies.

At hour 3.6, Figure C.2 (b) shows that the three output variables begin to change due to the second anomaly. The heating fluid temperature decreases again, the measured mix temperature does not change, and the measured volume does not change. Table C.2 shows the pattern and size of the second anomaly which matches the pattern of model $NF_{1,8}$, so we isolate the anomaly as faulty volume sensor fault, the 8th anomaly of the ten anomalies. These two anomalies have different patterns and sizes, so we can isolate this sequential faults after they occur.

Appendix D

Complementary Results of Neuro-Fuzzy Identification for Arbitrary Fault Size

D.1 Identifying the Faults

In this section, we use the Neuro-Fuzzy model to identify the anomalies by applying different fault size changes. The following results illustrate another example.

In Figure D.1 , the *star* variables indicate the symptoms of $F1$*: Mix Inflow Disturbance*, the *circle* variables indicate the symptom of $F6$*: Faulty Outflow Valve*, and the *plus* variables indicate the NF model in normal condition. Table D.1 shows the symptoms of $F1$ and $F6$ anomalies for ten fault size cases (These cases are combined in the figures and tables to save space). As before, each "symptom" is defined by two values, which are shown in Table D.1.

For the heating fluid temperature variable, Figure D.1(a) and Table D.1 show its pattern sizes. $F1$ and $F6$ have different pattern sizes for all fault sizes.

For the measured mix temperature variable, Figure D.1(b) and Table D.1 show its pattern sizes. $F1$ and $F6$ have similar pattern sizes at fault sizes ± 0.2, but have different pattern sizes for other fault sizes.

For the measured volume variable, Figure D.1(c) and Table D.1 show its pattern sizes. $F1$ and $F6$ have different pattern sizes for all fault sizes.

We need to consider the three output variables to isolate the two anomalies. As the heating fluid temperature and measured volume variables have totally different pattern sizes for $F1$ and $F6$ for all fault size cases, we can isolate $F1$*: Mix Inflow Disturbance* and $F6$*: Faulty Outflow Valve*.

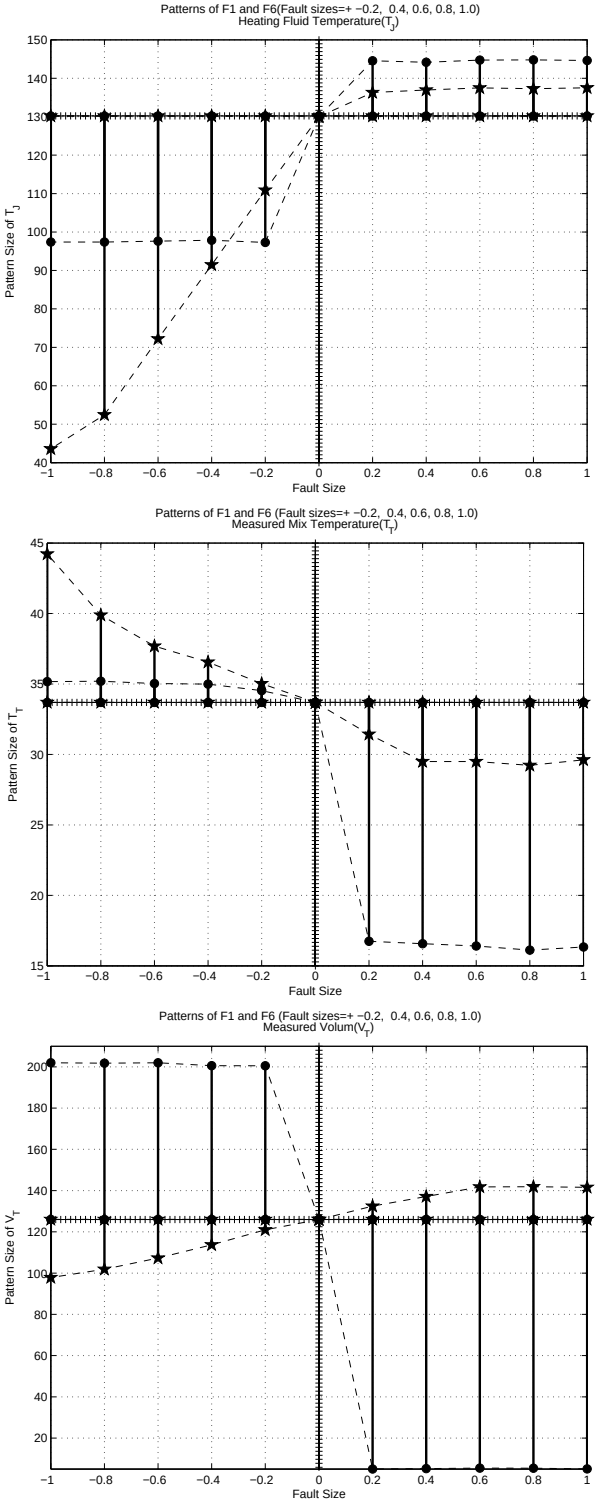

Figure D.1: Output Variable Patterns for $F1$ and $F6$

Fault Isolation Stage for $F1$ and $F6$						
	Heating Fluid Temperature $P(T_J) = [\,T_{J0} \quad T_{Jmax}\,]$ or $P(T_J) = [\,T_{Jmin} \quad T_{J0}\,]$, $^\circ C$		Measured Mix Temperature $P(T_T) = [\,T_{T0} \quad T_{Tmax}\,]$ or $P(T_T) = [\,T_{Tmin} \quad T_{T0}\,]$, $^\circ C$		Measured Volume $P(V_T) = [\,V_{T0} \quad V_{Tmax}\,]$ or $P(V_T) = [\,V_{Tmin} \quad V_{T0}\,]$, m^3	
Anomaly	Fault Size	Pattern Size	Fault Size	Pattern Size	Fault Size	Pattern Size
$F1$	-0.2	[130.1909 110.9066]	-0.2	[33.6885 35.0253]	-0.2	[120.9763 126.0445]
$F1$	-0.4	[130.1909 91.4607]	-0.4	[33.6885 36.5525]	-0.4	[113.698 126.0445]
$F1$	-0.6	[130.1909 72.2061]	-0.6	[33.6885 37.6848]	-0.6	[107.3168 126.0445]
$F1$	-0.8	[130.1909 52.4649]	-0.8	[33.6885 39.8864]	-0.8	[101.8772 126.0445]
$F1$	-1.0	[130.1909 43.6067]	-1.0	[33.6885 44.2223]	-1.0	[97.8262 126.0445]
$F1$	0.2	[130.1909 136.3023]	0.2	[31.4334 33.6885]	0.2	[126.0445 132.4546]
$F1$	0.4	[130.1909 136.9372]	0.4	[29.4955 33.6885]	0.4	[126.0445 137.1152]
$F1$	0.6	[130.1909 137.5039]	0.6	[29.4974 33.6885]	0.6	[126.0445 141.7853]
$F1$	0.8	[130.1909 137.291]	0.8	[29.2291 33.6885]	0.8	[126.0445 141.8658]
$F1$	1.0	[130.1909 137.5116]	1.0	[29.6192 33.6885]	1.0	[126.0445 141.5723]
$F6$	-0.2	[97.299 130.1909]	-0.2	[33.6885 34.5268]	-0.2	[126.0445 200.5301]
$F6$	-0.4	[97.8644 130.1909]	-0.4	[33.6885 34.9905]	-0.4	[126.0445 200.5769]
$F6$	-0.6	[97.6249 130.1909]	-0.6	[33.6885 35.0284]	-0.6	[126.0445 201.9522]
$F6$	-0.8	[97.3916 130.1909]	-0.8	[33.6885 35.1977]	-0.8	[126.0445 201.7956]
$F6$	-1.0	[97.3982 130.1909]	-1.0	[33.6885 35.1683]	-1.0	[126.0445 201.9857]
$F6$	0.2	[130.1909 144.5512]	0.2	[16.7401 33.6885]	0.2	[5.032 126.0445]
$F6$	0.4	[130.1909 144.1619]	0.4	[16.5693 33.6885]	0.4	[5.2079 126.0445]
$F6$	0.6	[130.1909 144.7405]	0.6	[16.4106 33.6885]	0.6	[5.4762 126.0445]
$F6$	0.8	[130.1909 144.7842]	0.8	[16.1144 33.6885]	0.8	[5.4103 126.0445]
$F6$	1.0	[130.1909 144.6244]	1.0	[16.335 33.6885]	1.0	[5.0811 126.0445]

Table D.1: Fault Isolation Stage for $F1$ and $F6$

D.2 Neuro-Fuzzy Model Practical Application

D.2.1 Producing Data Using the JCSTR System

For a real world plant, we use the fault-free Neuro-Fuzzy models to identify all the faults. This can eliminate the difficulty of having to train a bank of NF models for all fault scenarios using plant data. The anomaly *F7: Faulty Heating Fluid Inflow Valve Fault* is given as another example to show the method and results. Figures D.2, the *circle* variables indicate the outputs symptoms produced using the Neuro-Fuzzy faulty model. The *star* variables indicate the output symptoms produced using the Neuro-Fuzzy fault-free model. The *plus* variable indicates NF model in normal condition.

In Table D.2, NF_7 indicates the NF faulty heating fluid inflow valve model, and NF_0 indicates the NF fault-free model. The results show that they have very similar pattern sizes. Thus, using the Neuro-Fuzzy fault-free model, we can still identify the anomalies.

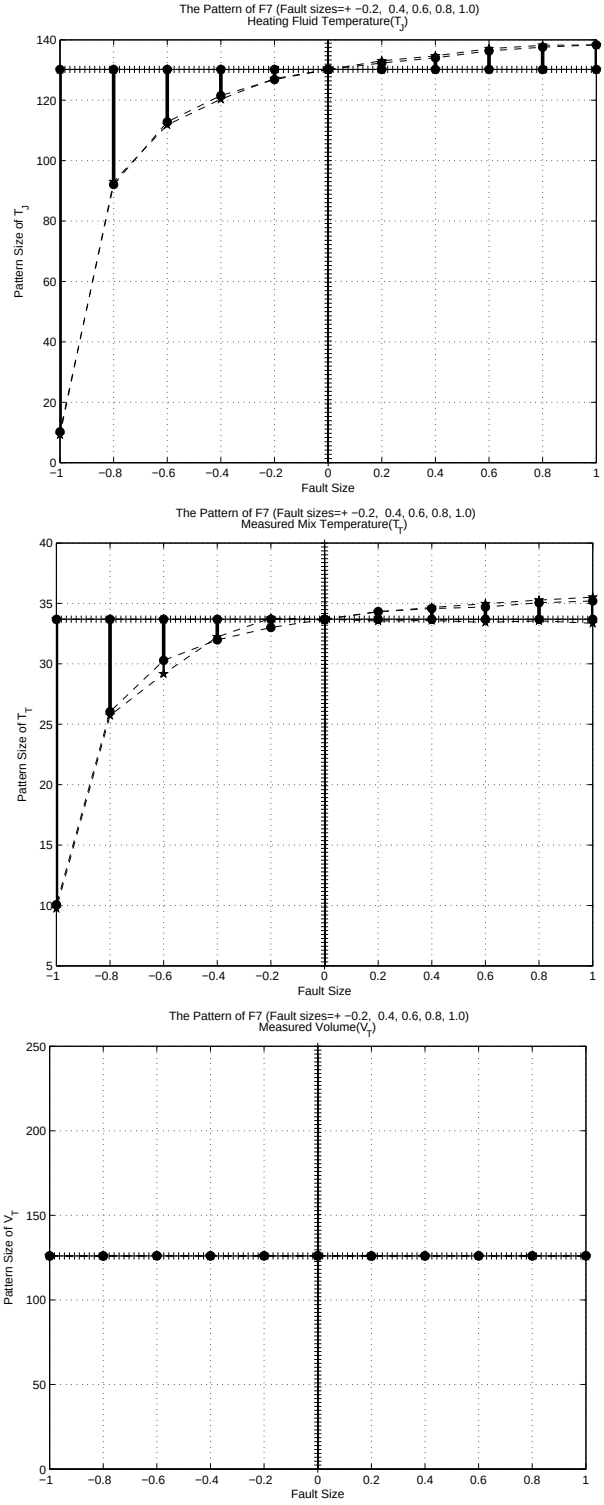

Figure D.2: Output Variable Patterns for $F7$

Fault Isolation Stage for Fault-free Model NF_0 and Faulty Model NF_7						
	Heating Fluid Temperature $P(T_J) = [\,T_{J0} \quad T_{Jmax}\,]$ or $P(T_J) = [\,T_{Jmin} \quad T_{J0}\,]$, $^\circ C$		Measured Mix Temperature $P(T_T) = [\,T_{T0} \quad T_{Tmax}\,]$ or $P(T_T) = [\,T_{Tmin} \quad T_{T0}\,]$, $^\circ C$		Measured Volume $P(V_T) = [\,V_{T0} \quad V_{Tmax}\,]$ or $P(V_T) = [\,V_{Tmin} \quad V_{T0}\,]$, m^3	
NF Model	Fault Size	Pattern Size	Fault Size	Pattern Size	Fault Size	Pattern Size
NF_7	-0.2	[126.8499 130.1909]	-0.2	[33.0051 33.6885]	-0.2	[126.0445 126.0611]
NF_7	-0.4	[121.5481 130.1909]	-0.4	[31.9813 33.6885]	-0.4	[126.0112 126.0445]
NF_7	-0.6	[112.8213 130.1909]	-0.6	[30.2849 33.6885]	-0.6	[126.1042 126.0445]
NF_7	-0.8	[92.0940 130.1909]	-0.8	[26.0341 33.6885]	-0.8	[125.9017 126.0445]
NF_7	-1.0	[10.2109 130.1909]	-1.0	[10.0619 33.6885]	-1.0	[125.9563 126.0445]
NF_7	0.2	[130.1909 133.1452]	0.2	[33.6885 34.3217]	0.2	[125.8826 126.0445]
NF_7	0.4	[130.1909 134.0199]	0.4	[33.6885 34.5756]	0.4	[125.9560 126.0445]
NF_7	0.6	[130.1909 136.3253]	0.6	[33.6885 34.7037]	0.6	[126.0445 126.0595]
NF_7	0.8	[130.1909 137.5921]	0.8	[33.6885 35.0510]	0.8	[126.0232 126.0445]
NF_7	1.0	[130.1909 138.3256]	1.0	[33.6885 35.1985]	1.0	[126.0445 126.0948]
NF_0	-0.2	[127.1545 130.1909]	-0.2	[33.7770 33.6885]	-0.2	[126.0445 126.1232]
NF_0	-0.4	[120.3331 130.1909]	-0.4	[32.2322 33.6885]	-0.4	[126.0445 126.1773]
NF_0	-0.6	[111.8213 130.1909]	-0.6	[29.1643 33.6885]	-0.6	[126.0445 126.2174]
NF_0	-0.8	[93.0364 130.1909]	-0.8	[25.7273 33.6885]	-0.8	[126.0445 126.0573]
NF_0	-1.0	[9.2182 130.1909]	-1.0	[9.7511 33.6885]	-1.0	[126.0445 126.1296]
NF_0	0.2	[130.1909 132.3659]	0.2	[33.6885 34.3102]	0.2	[125.9598 126.0445]
NF_0	0.4	[130.1909 133.6348]	0.4	[33.6885 34.6608]	0.4	[126.0445 126.1612]
NF_0	0.6	[130.1909 135.4073]	0.6	[33.6885 34.9781]	0.6	[126.0445 126.1608]
NF_0	0.8	[130.1909 137.0429]	0.8	[33.6885 35.2796]	0.8	[126.0445 126.1512]
NF_0	1.0	[130.1909 137.8317]	1.0	[33.6885 35.5141]	1.0	[125.9191 126.0445]

Table D.2: Fault Isolation Stage for NF_0 and NF_7

VITA

Candidate's full name: Jing He

Universities attended: Bachelor in Electrical Engineering,
Tianjin Institute of Technology, 1994

Publications:

Conference Presentations: